

Typology of extreme flood event leads to differential impacts on soil functioning

Rafael Sanchez-Rodriguez, Antonio; Hill, Paul W.; Chadwick, David R.; Jones, Davey L.

Soil Biology and Biochemistry

DOI:
[10.1016/j.soilbio.2018.11.019](https://doi.org/10.1016/j.soilbio.2018.11.019)

Published: 01/02/2019

[Cyswllt i'r cyhoeddiad / Link to publication](#)

Dyfyniad o'r fersiwn a gyhoeddwyd / Citation for published version (APA):
Rafael Sanchez-Rodriguez, A., Hill, P. W., Chadwick, D. R., & Jones, D. L. (2019). Typology of extreme flood event leads to differential impacts on soil functioning. *Soil Biology and Biochemistry*, 129, 153-168. <https://doi.org/10.1016/j.soilbio.2018.11.019>

Hawliau Cyffredinol / General rights

Copyright and moral rights for the publications made accessible in the public portal are retained by the authors and/or other copyright owners and it is a condition of accessing publications that users recognise and abide by the legal requirements associated with these rights.

- Users may download and print one copy of any publication from the public portal for the purpose of private study or research.
- You may not further distribute the material or use it for any profit-making activity or commercial gain
- You may freely distribute the URL identifying the publication in the public portal ?

Take down policy

If you believe that this document breaches copyright please contact us providing details, and we will remove access to the work immediately and investigate your claim.

1 **Typology of extreme flood event leads to differential impacts on soil functioning**

2 Antonio Rafael Sánchez-Rodríguez^{a,b,*}, Paul W. Hill^a, David R. Chadwick^a, Davey L. Jones^{a,c}

3 ^a *School of Environment, Natural Resources and Geography, Environment Centre Wales,*
4 *Bangor University, Gwynedd LL57 2UW, UK*

5 ^b *Departamento de Agronomía, Universidad de Córdoba, ETSIAM, Córdoba, Andalucía*
6 *14071, Spain*

7 ^c *UWA School of Agriculture and Environment, University of Western Australia, Crawley, WA*
8 *6009, Australia*

9

10 *Corresponding author. Tel.: +44 1248 383052; fax: +44 1248 354997.

11 E-mail address: antonio.sanchez@uco.es (A.R. Sánchez-Rodríguez).

12

13 **ABSTRACT**

14 Soils around the world are being exposed to weather events which are unprecedented in recent
15 history. To maintain the delivery of soil-related ecosystem services and to promote greater
16 soil resilience it is essential to understand how plant-soil systems respond to these extreme
17 events. In this study we replicated a recent period of extreme rainfall and prolonged spring
18 flooding in a temperate grassland which had no previous history of flooding. Intact soil
19 mesocosms (Eutric Cambisol) 1 kg weight were subjected to a simulated long-term spring
20 flood (15°C, 2 months) and maintained in the light with above ground indigenous vegetation
21 (*Lolium perenne* L.) or dark with and without indigenous vegetation to simulate different
22 flood typologies. In comparison to a no-flood control treatment, nutrient cycling, water
23 quality, air quality (greenhouse gas emissions), habitat provision and biological population
24 regulation shifts were evaluated. Flooding induced a rapid release of nutrients into the soil
25 solution and overlying floodwater, resulting in potential nutrient losses up to 15 mg Fe, 16 mg
26 NH₄⁺, 360 mg DOC and 28 mg DON, per mesocosm. The presence of plants increased the

27 rate of nutrient release (especially P), with the effects magnified when light transmission
28 through the floodwater was restricted (1.3 mg P vs 0.2 mg P, per mesocosm). Flooding
29 induced a rapid decline in redox potential and subsequent production of CH₄, especially in the
30 darkened treatments (10 and between 11–16 times higher than the control, without and with
31 light restrictions, respectively). Upon removal of the floodwater, the accumulated NH₄⁺ was
32 nitrified leading to a shift in greenhouse gas emissions, from CH₄ to N₂O emissions. N₂O was
33 only significantly produced in the mesocosms kept under light restrictions (13 times higher
34 than in other two treatments). Flooding eliminated earthworms, reduced grass production after
35 soil recovery (from 28 g for control mesocosms to 11 g and < 1 g for flooded mesocosms
36 without and with light restrictions, respectively). Soil microbial biomass was also reduced (up
37 to a 22–27 % of the total PLFAs) and flooding induced shifts in microbial community
38 structure, particularly a loss of soil fungi. The soil fungi content quickly recovered (4 weeks)
39 when light was not restricted during the flood period, however, no such recovery was seen in
40 the darkened treatments. Overall, we conclude that extreme flood events cause rapid and
41 profound changes in soil function. Both the impact of the flooding and the time to recover is
42 exacerbated when light is restricted (e.g. in sediment laden floodwater). In addition, our
43 results suggest that the presence of flood-resilient plants can mitigate against some of the
44 negative impacts of flooding on soil functioning.

45

46 **Keywords:** Climate change, nitrate, PLFA profiling, tipping point, waterlogging tolerance,

47 ³³P

48 **1. Introduction**

49 Against a backdrop of progressive climate change, there is increasing evidence that many
50 ecosystems are also experiencing more extremes in weather (e.g. heat, droughts, floods and
51 ground level ozone; Easterling et al., 2000). Within Western Europe, recent quasi-stochastic
52 extremes in air temperature and changes in the periodicity and intensity of rainfall have been
53 directly linked to climate change (Allan, 2011; Pall et al., 2011; Jones et al., 2012). To a large
54 extent this appears to be due to behavioural changes in the North Atlantic oscillation weather
55 system which is influenced by the polar vortex and Pacific jet stream (Murphy et al., 2009).
56 Alterations in this weather system have now been linked to numerous unprecedented storms
57 and long-term flooding events within the UK (Met Office, 2014). Examples of these include
58 those seen in the summer of 2012 and in the winter of 2013-2014 when large areas within the
59 England and Wales remained flooded for 10-12 weeks, in some cases under several metres of
60 floodwater (McEwen et al., 2014). Although some of these areas clearly lie within flood
61 plains which have a long history of inundation, importantly, other areas with no previous
62 documented history (>150 years) of flooding were also affected (Clout, 2014; Thorne, 2014).
63 These agroecosystems were severely impacted by the long-term flooding, typically resulting
64 in complete crop failure, loss of soil functions and in some cases a complete loss of topsoil
65 due to water erosion (Natural England, 2014). After the floodwater receded, it was also
66 apparent that there was a lack of appropriate interventions to reverse the negative impacts on
67 soil functioning as the impacts of extreme flooding were poorly understood. There is therefore
68 a clear need to understand the impact of extreme precipitation events on the soils with no
69 previous history of flooding.

70 Depending on the typology of the flood event, i.e. duration, depth, origin of the water
71 (Sánchez-Rodríguez et al., 2018), and the soil/vegetation combination, prolonged inundation
72 is expected to impact upon soil functions to different extents. Bünemann et al. (2018) has
73 recently reviewed the multiple aspects and definitions of soil quality. In this manuscript, we

74 define soil quality as “the capacity of a soil to function within ecosystem and land-use
75 boundaries to sustain biological productivity, maintain environmental quality, and promote
76 plant and animal health” (Doran and Parkin, 1994, 1996). While short term flooding (<7 d)
77 may have limited impact on soil functions, extreme flood events (> 2 months) may have
78 major consequences on the delivery of a range of ecosystem services both during the flood
79 itself and during the recovery phase (Niu et al., 2014), such as biomass production,
80 biodiversity and water quality and supply. These soil-based ecosystem services are associated
81 with soil functions, including habitat provision for roots and soil organisms, element cycling,
82 decomposition, maintenance of soil structure, regulation of biological populations, water
83 cycling and organic matter cycling (Bünemann et al., 2018).

84 After a few weeks of flooding, anaerobic conditions prevail in flooded grassland soils,
85 facilitating the solubilisation of reduced elements (e.g. Fe, Mn; Schalinghe et al., 2007) and
86 alterations in nutrient (P, Fe, N, C) cycles, including the release of soluble C and N (Jones et
87 al., 2009) and promoting the loss of nutrients (via leaching or to the overlying water column).
88 In addition, light ingress can be reduced preventing photosynthesis and inducing plant
89 senescence (Mommer et al., 2005a; Shaw et al., 2013) depending upon the nature of the
90 floodwater (particles suspended within the water column and deposited onto the foliage
91 surface). Under these anaerobic conditions certain greenhouse gas (GHG) emissions could be
92 stimulated; CH₄ production and N₂O emissions related to denitrification (transformation of
93 NO₃⁻ to N₂O/N₂ mediated by soil bacteria) are anticipated (Hou et al., 2000), but N₂O
94 production due to nitrification (transformation of NH₄⁺ to NO₃⁻ mediated by soil bacteria)
95 will be reduced as it is an aerobic process (Norton, 2008). These conditions facilitate the
96 decomposition of organic matter derived from the senescing plant material and obligate-
97 aerobic components of the microbial community. Soil microbial communities and some soil
98 microorganisms, e.g. fungi, could be negatively affected if the inundation is prolonged, while
99 other taxonomic groups, e.g. Gram⁺ bacteria, may prove more resistant (Ferré et al., 2012).

100 Phospholipid-derived fatty acids (PLFAs) as bioindicators of different taxonomic groups have
101 been traditionally used to assess these alterations in microbial communities of flooded soils
102 (Bossio and Scow, 1998). Finally, eutrophication of water bodies and a decline in soil
103 functionality and associated ecosystem services are expected after a prolonged flooding event
104 (Scalenghe et al., 2012; Brun and Barros, 2013; Shaw et al., 2013).

105 Until now, flooding experiments have largely focused on the options to mitigate flood
106 risk. They have usually been short term laboratory studies with disturbed soil, without
107 vegetation and non-extreme flooding, as reviewed by Brun and Baros (2013) and Shaw et al.
108 (2013). There is a lack of information about the magnitude of long-term flooding and its
109 effects on agricultural grasslands. Therefore, more realistic mesocosm experiments are needed
110 to better understand soil ecosystem responses during and after extreme flood events, and to
111 help develop strategies to minimize the effects of these events on agricultural land.

112 The main aim of this study was to evaluate the impact of different types of extreme flood
113 event (9 weeks) on soil functioning within intact soil mesocosms with and without indigenous
114 vegetation to reflect different possibilities that can occur in nature, in comparison with non-
115 flooded mesocosms. Four different flood typologies were designed to separate the influence
116 of above-ground and below-ground processes (i.e. flooded soil cores with indigenous
117 vegetation versus flooded soil cores without indigenous vegetation) and to simulate the
118 presence or absence of turbid floodwater (i.e. dark versus light conditions). Specifically, we
119 addressed: (i) alterations in element cycling and water quality (Fe, P, N, C) during the
120 extreme flood event (9 weeks) and 5 weeks of soil recovery, air quality (GHG emissions),
121 habitat provision and biological population regulation during 5 weeks after the floodwater
122 was removed (changes in soil microbial community structure, number of earthworms); and
123 (ii) the relation between the cause of these alterations (flood typology), soil parameters and
124 GHG emissions. We hypothesised that (i) flood types in which the availability of light is
125 restricted will result in a greater loss of soil functionality due to negative feedbacks caused by

126 the death of the vegetation, and (ii) a part of the indigenous vegetation will survive when the
127 light is not restricted and will be key to maintaining soil function during and after flooding.

128

129 **2. Materials and methods**

130 *2.1 Soil sampling and soil properties*

131 Sixteen intact soil samples were collected directly from the surface Ah horizon (0-10
132 cm) of a sheep-grazed, *Lolium perenne* L. dominated, low intensity grassland, located in
133 Abergwyngregyn, Gwynedd, North Wales (53°14'21"N, 4°00'57"W) in October 2014. The
134 soil samples, which consisted of 100 cm³ blocks, were removed intact with associated
135 vegetation (sward height ca. 4 cm). The soil is classified as a sandy clay loam textured Eutric
136 Cambisol with fine crumb structure as detailed in Palomo et al. (2006) and summarized in
137 Table S1. The soil receives an annual fertiliser dose of 100 kg N ha⁻¹, 20 kg K ha⁻¹ and 20 kg
138 P ha⁻¹.

139 Soil electrical conductivity (EC) and pH were determined in 1:1 (v/v) soil: distilled
140 H₂O extracts (Smith and Doran, 1996). Calcium carbonate (CaCO₃) was determined by the
141 Van Slyke manometric method (Nelson, 1982). Exchangeable cations (Na, K, Ca, Mg and Al)
142 were extracted by shaking (1 h, 20°C) using a 1:10 (w/v) soil:0.5 M BaCl₂ extract with
143 subsequent cation analysis using a Series 720 ICP-OES (Agilent Technologies Inc., Santa
144 Clara, CA). Available P was quantified in a 1:5 (w/v) soil:0.5 M acetic acid extract (1 h, 200
145 rev min⁻¹) with subsequent P analysis by the molybdate blue method of Murphy and Riley
146 (1962). A CHN-2000 analyser (Leco Corp., St Joseph, MI) was used to determine total
147 organic carbon (C) and nitrogen (N) in soil. NO₃⁻ and NH₄⁺ in soil solution were extracted
148 according to Giesler and Lundström (1993) and determined with a Skalar San⁺ segmented
149 flow analyser (Skalar UK Ltd, York, UK).

150

151 *2.2. Experimental design and treatments*

152 Immediately after collection from the field, the intact soil blocks (ca. 1 kg) were
153 placed at the bottom of transparent 110 × 80 × 270 mm (l × w × h) polypropylene containers.
154 The top of the containers were left open to facilitate gas exchange. No drainage holes were
155 placed in the base. The containers were transferred to a climate-controlled Fitotron[®] plant
156 growth chamber (Weiss Technik UK Ltd, Ebbw Vale, UK) with photoperiod of 16 h day⁻¹,
157 light intensity of 350 μmol m⁻² s⁻¹, temperature of 15°C and relative humidity of 70 %. A
158 single Rhizon[®] sampler (Rhizosphere Research Products, Wageningen, Netherlands) was
159 inserted into the centre of each soil block to non-destructively recover soil solution. To label
160 the plant-available P pool, 100 ml of a solution containing ³³P (H₃³³PO₄, 111 TBq mmol⁻¹;
161 1.23 kBq ml⁻¹; American Radiolabeled Chemicals Inc., St Louis, MO) was evenly applied to
162 the soil surface of each container two weeks before the flooding started.

163 The experiment had four distinct stages:

164 *1. Pre-flood stage:* This initial phase involved placing each plant-soil mesocosm (*n* = 16)
165 into the growth chamber for 2 weeks to allow acclimation. The soils were maintained field-
166 moist by the daily addition of oligotrophic river water (collected from the Aber River adjacent
167 to where the soil samples were collected) based on their weight loss. This also permitted ³³P
168 to become re-distributed within the plant-microbial-soil system;

169 *2. Flood stage:* This phase incorporated the four main flood treatments alongside an
170 unflooded control treatment (maintained at field-moist based on weight loss), namely:

171 T₁: flooded soil with no above-ground vegetation and maintained in the dark [flood+dark
172 (no veg.) treatment]

173 T₂: flooded soil with above-ground vegetation and maintained in the dark (flood+dark
174 treatment)

175 T₃: flooded above-ground vegetation (from T₁) with no soil and maintained in the dark
176 [flood+dark (only veg.) treatment]

177 T₄: flooded soil with above-ground vegetation and maintained in the light (flood+light
178 treatment)

179 T₅: unflooded soil with above-ground vegetation and maintained in the light
180 (control+light treatment)

181 Firstly, the vegetation from 4 replicate containers was cut at ground level (T₁) and the
182 grass clippings transferred to 4 new containers containing no soil (T₃), increasing the number
183 of containers up to 20. Secondly, river water was used to flood 16 of the containers (T₁-T₄),
184 including the four in which the grass was cut to soil level, and the four containing grass only.
185 Each container received ca. 1200 ml of river water to achieve a flood height of 10 cm above
186 the soil surface (reflecting typical flood depths observed in the region during extreme weather
187 events; Figs. S1-S3). Twelve containers were subsequently covered by black plastic prevent
188 light entry into the microcosms (T₁-T₃). Four microcosms were left unflooded and exposed to
189 the light as a control (T₅). The floodwater was maintained at a constant height throughout the
190 experiment through the addition of river water, while the unflooded control treatments were
191 maintained field-moist as in the pre-flood phase. This phase lasted for 9 weeks.

192 *3. Soil recovery stage:* At this point in the experiment the flood water was carefully
193 removed from treatments T₁-T₄. All treatments were then exposed to the light and ambient air
194 and allowed to dry out naturally. This stage had a duration of 5 weeks and aimed to simulate
195 the period before which agronomic practices recommenced.

196 *4. Soil functions assessment stage:* To evaluate any legacy effects of the flooding on
197 soil functioning, a pot-based bioassay was performed. Briefly, 500 g of soil was recovered
198 from each treatment (with roots removed) and placed in a 500 cm³ pot and sown with two 3 d-
199 old maize seedlings (*Zea mays* L.). The pots were placed in the same growth chamber as used
200 above for 28 d, except that the temperature was maintained at 20 °C. Thirty ml of a solution
201 containing N, P and K (10 mM KNO₃, 15 mM KH₂PO₄) were applied on a weekly basis to
202 remove nutrient limitation. After 7 d, one plant from each pot was removed. The pots were

203 weighed and watered with river water 3 times per week to maintain the soils in a field-moist
204 condition.

205

206 *2.3. Measurement of soil chemical and biological indicators*

207 *2.3.1. Element cycling and water quality*

208 Depending upon treatment and experimental stage, soil solution and floodwaters were
209 collected approximately weekly and analysed for pH, electrical conductivity (EC), total Fe
210 (Loeppert and Inskeep, 1996), Fe^{2+} (Loeppert and Inskeep, 1996), P (Murphy and Riley,
211 1962), ^{33}P , NO_3^- (Miranda et al., 2001), NH_4^+ (Mulvaney, 1996), total dissolved N (TDN) and
212 dissolved organic C (DOC). Additional samples were taken the day before and after the first
213 and the last days of the flood stage. Fe, P, NO_3^- and NH_4^+ were determined by
214 spectrophotometry on a PowerWave XS microplate reader (BioTek Instruments Inc.,
215 Winooski, VT). TDN and DOC were determined using a Multi N/C 2100/2100 analyser
216 (AnalytikJena AG, Jena, Germany). Dissolved organic N (DON) was calculated by
217 subtraction of NO_3^- and NH_4^+ from the TDN value. ^{33}P in solution was determined by liquid
218 scintillation counting on a Wallac 1404 scintillation counter (Wallac EG&G, Milton Keynes,
219 UK) after mixing with Optiphase Hisafe 3 scintillation fluid (PerkinElmer Inc., Waltham,
220 MA). Soil redox potential was determined periodically through the experiment using a
221 SenTix[®] probe (WTW Wissenschaftlich-Technische Werkstätten GmbH, Weilheim,
222 Germany) inserted in the surface of the soil (0-3 cm depth).

223 During the flood stage, the total amount of nutrient released into the soil solution and
224 overlying floodwater (C_{release}) was calculated as follows:

$$225 \quad C_{\text{release}} \text{ (mg container}^{-1}\text{)} = [C_{\text{sol}} \times V_{\text{soil}} \times \Theta] + [C_{\text{flood}} \times V_{\text{flood}}] \quad \text{(Eqn. 1)}$$

226 where C_{sol} and C_{flood} are the concentration of nutrient in the soil solution and floodwater
227 respectively, V_{soil} and V_{flood} are the volume of soil and floodwater respectively and Θ is the
228 volumetric water content ($0.5 \text{ cm}^3 \text{ cm}^{-3}$).

229

230 2.3.2. *Air quality*

231 Although some small N₂O emissions from residual soil NO₃⁻ at the start of flooding
232 were detected in a similar previous experiment (Sánchez-Rodríguez et al., 2017), the most
233 important emissions were measured during the soil recovery phase (Sánchez-Rodríguez et al.,
234 2017, 2018). This is the reason why we focused our GHGs measurements on the soil recovery
235 stage. On the last day of the flood stage and through the flood recovery stage the mesocosms
236 were hermetically sealed during the samplings (the day before the floodwater was removed,
237 the same day after the floodwater was removed and weekly until the end of the soil recovery).
238 At 0 h and 1 h after sealing (between 10.00 h and 12.00 h), 20 ml of headspace gas was
239 removed using a hypodermic syringe via a rubber septum placed in the mesocosm lid, and the
240 gas transferred to a pre-evacuated glass vial. CH₄, CO₂ and N₂O concentrations in the vials
241 were subsequently analysed by gas chromatography using a Clarus 500 GC equipped with a
242 HS-40Turbomatrix headspace analyser, ⁶³Ni electron-capture detector and flame ionization
243 detector connected to a methanizer (PerkinElmer Inc.). Fluxes were estimated as the
244 difference in gas concentration at time 0 and 1 h and after correction for both temperature and
245 the ratio between chamber volume and soil surface area (MacKenzie et al., 1998). Cumulative
246 fluxes were estimated by linear interpolation, multiplying the mean of two successive daily
247 fluxes by the number of hours between the two measurements and adding that amount to the
248 previous cumulative total.

249 2.3.3. *Habitat provision and biological population regulation*

250 At the end of the soil recovery stage (second phase of the experiment), the dry weight of grass
251 and number of earthworms per box were weighed and counted, respectively. Maize plant
252 height was measured after 14 and 28 d, plant dry weight was determined (80 °C, 72 h) and
253 mineral element concentrations in above- and below-ground biomass determined by ICP-OES
254 after dry-ashing and digestion with hydrochloric acid (Adrian, 1973) at the end of the soil

255 functions assessment stage (fourth phase of the experiment), To evaluate changes in microbial
256 community structure, soil samples (25 g) from each container were collected at the beginning
257 and at the end of soil recovery stage and stored at -80°C for PLFA analysis and subsequently
258 determined as described in Bartelt-Ryser et al. (2005). Although a total of 50 fatty acids were
259 identified in the soil samples, Table 1 shows the 23 with a concentration higher than 0.5% of
260 the total PLFAs that were used as biomarkers for the different taxonomic groups according to
261 Ratledge and Wilkinson (1988), Bedard and Knowles (1989), Bowman et al. (1991, 1993),
262 Kieft et al. (1994), Paul and Clark (1996), Bossio and Scow (1998), Olsson et al. (1999),
263 Zelles (1999), Niklaus et al. (2003), Bartelt-Ryser et al. (2005) and using standard
264 nomenclature as described in Frostegård et al. (1993). Despite their known limitations
265 (Frostegård, 2011), the following PLFA biomarker ratios were calculated: fungi-to-bacteria as
266 an indicator of large scale community shifts, predator-to-prey (protozoa/bacteria) to estimate
267 the availability of nutrients to support higher trophic levels, Gram+-to-Gram- as an indicator
268 of soil aeration state (Bossio and Scow, 1998), saturated-to-unsaturated fatty acids (sat/unsat)
269 as an indicator of the stability of the microbial community, mono-to-polyunsaturated fatty
270 acids (mono/poly), precursor-to-cyclopropane fatty acids (precursor/cyclopropane fatty acids;
271 16 ω /17 cyclo and 18 ω /19 cyclo) as indicators of high stress (Knivett and Cullen, 1965).

272

273 *2.4. Statistical analysis*

274 Repeated measured analysis of variance (RM of ANOVA) based on a completely
275 randomized design with 4 treatments and 4 replications per treatment were applied to pH, EC,
276 Fe, P, ³³P, NH₄⁺, NO₃⁻, DON, DOC in soil solution [flood+dark (no veg.), flood+dark,
277 flood+light and control+light] and flood water [flood+dark (no veg.), flood+dark, flood+dark
278 (only veg.) and flood+light] as well as for soil redox potential and daily GHG emissions
279 during the soil recovery stage [flood+dark (no veg.), flood+dark, flood+light and
280 control+light]. Bonferroni multiple comparison test at a probability level of 0.05 was used to

281 identify differences between treatments. ^{33}P (‰) is expressed as the ^{33}P of the sample / ^{33}P of
282 the original radioactive solution (accounting for radioactive decay) \times 1000 for soil solution
283 samples and, additionally, multiplying by 13 only in the case of floodwater samples, because
284 the initial 100 ml of radioactive solution (applied to the soil of all containers) were diluted
285 when 1.2 l of fresh water were applied to flood+dark (no veg.), flood+dark and flood+light
286 containers at the beginning of the flood-stage.

287 Analysis of variance (ANOVA) based on a completely randomized design with the
288 same number of treatments and replications was applied to the plant biomass, plant nutrient
289 content, earthworm, cumulative GHG, and PLFA data. In these cases, Tukey's HSD *post hoc*
290 was used to identify treatment differences.

291 To identify relationships between soil microbial communities and GHG daily fluxes,
292 soil redox potential, NO_3^- and NH_4^+ in soil solution, and to find differences between
293 treatments, principal component analysis (PCA) was performed at the end of the flood and
294 soil recovery stages, based on a data correlation matrix to elucidate differences between
295 treatments. Finally, Pearson correlations were carried out between these parameters using the
296 data obtained during the soil recovery. The statistical analyses were performed using the
297 statistical package SPSS software v22.0 (IBM Inc., Armonk, NY).

298

299 **3. Results**

300 *3.1. Element cycling and water quality: Response of soil chemical indicators to extreme* 301 *flooding*

302 Few major treatment effects were observed in soil solution pH, however, slightly
303 higher soil solution pH values were obtained in the flood treatments [flood+dark(no veg.),
304 flood+dark and flood+light] relative to the control+light treatment 3-5 weeks after flooding
305 (Fig. 1a). The floodwater (Fig. 1b), pH values were similar to those of soil, with the exception
306 of the flood+light treatment (T_4) which had a significantly higher pH relative to the dark-flood

307 treatments (T_1 and T_2). In contrast to pH, major changes in soil EC and redox potential in
308 response to flooding were observed (Fig. 1c-e). In all flood treatments, soil solution EC
309 increased markedly during the experiment, especially during the flood stage, but quickly
310 declined at the soil recovery stage (Fig. 1c). The increase in EC was slower in the illuminated
311 flood treatment (T_4) relative to those maintained in the dark. In comparison to the soil, the EC
312 of the floodwater remained lower with the highest values seen in the treatments containing
313 soil and maintained in the dark (Fig. 1d). Redox potential rapidly declined in the flood
314 treatments and then remained constant throughout the flood period (Fig. 1e). The redox
315 potential remained consistently higher in the illuminated flood treatments in comparison to
316 those maintained in the dark. After flood removal, the redox potential rapidly increased,
317 reaching positive values again within ca. 7 d and values close to the non-flooded treatment
318 control (T_5) by 21 d.

319 The dynamics of Fe^{2+} (not shown) in soil solution and floodwater exhibited a similar
320 temporal pattern to total Fe (Fig. 2ab) and represented 60% of the total Fe in soil solution and
321 65% of total Fe in flood water (averaged across the whole flooding period). Fe concentrations
322 in soil solution rapidly increased after commencement of the flood treatment (albeit slower in
323 T_4 relative to T_1 and T_2), peaking at ≈ 29 mg Fe l^{-1} at the end of flood stage (Fig. 2a). In
324 comparison, soil solution Fe concentrations in the control treatment (T_5) remained low
325 throughout the experiment. After flood removal, soil solution Fe in the flooded treatments
326 rapidly dropped to values similar to the control. Significant amounts of Fe accumulated in
327 floodwater albeit at lower concentration than observed in soil solution (Fig. 2b). Floodwater
328 Fe concentrations in the flooded treatments containing soil started to increase after 7 d,
329 reaching maximal values by week 4. In contrast, Fe concentrations remained very low when
330 no soil and only vegetation was present (T_3). The potential Fe lost (mg mesocosm $^{-1}$) was 14.8
331 ± 0.4 in T_1 [flood+dark (only veg.)], 14.9 ± 2.0 in T_2 (flood+dark) and 12.3 ± 0.6 in T_4
332 (flood+light), being 0.5 ± 0.1 from the grass in T_3 [flood+dark (only veg.)].

333 Phosphorus in soil solution remained low throughout the experiment (0.10 to 0.54 mg
334 l^{-1}). Although a simple explanation is not possible, several spikes in soluble P were seen
335 during the flood stage, however, few significant treatment effects were observed (Fig. 2c).
336 This is supported by the data obtained for ^{33}P which also showed a very low P concentration
337 and no significant differences between treatments (Fig. 2e). After flood removal, the amount
338 of ^{33}P in soil solution was negligible ($<0.1\%$ of the initial value). In contrast to soil solution,
339 significant increases in both P and ^{33}P were observed in floodwater (Fig. 2df). Floodwater P
340 concentrations were highest in treatments containing no soil (T_3 , grass only) and significantly
341 lower in the illuminated flood treatment (T_4). The calculated potential P loss from the soil (mg
342 mesocosm^{-1}) was 0.6 ± 0.2 in T_1 [flood+dark (no veg.)], 0.8 ± 0.2 in T_2 (flood+dark) and 0.2
343 ± 0.1 in T_4 (flood+light). This value was higher for T_3 (grass only) being 1.3 ± 0.2 mg
344 mesocosm^{-1} .

345 A similar pattern to Fe was observed for NH_4^+ during flooding (Fig. 3a). In the control
346 treatment (T_5), NH_4^+ concentrations remained low throughout the experiment (<0.7 mg l^{-1}).
347 The imposition of a flood, however, induced a progressive increase in NH_4^+ concentration
348 until the end of the flood stage. This was particularly evident in the flooded treatments
349 without light (T_1 , T_2) with NH_4^+ concentrations increasing immediately after flooding. When
350 light was present (T_4), a significant lag phase in NH_4^+ production occurred after flooding with
351 the concentrations being much less than in the dark treatments. After flood removal, the NH_4^+
352 concentrations initially fell in all treatments, however, this was greater when plants were
353 present in the mesocosms. NH_4^+ was only detected in the overlying floodwater in the dark
354 treatments (Fig. 3b). The calculated potential NH_4^+ lost (mg mesocosm^{-1}) was considerably
355 higher in T_1 [16.9 ± 2.0 , dark+flood (no veg.)] and T_2 (15.4 ± 1.0 , dark+flood) than in T_3 (2.7
356 ± 1.3 , dark+flood [only veg.]) and T_4 (4.3 ± 2.0 , light+flood).

357 The concentration of NO_3^- in soil solution was low in all treatments throughout the
358 flood stage (Fig. 3c). However, upon flood removal significant increases in NO_3^- were

359 observed, especially in those mesocosms which had been previously maintained in the dark.
360 In comparison to NH_4^+ , the levels of NO_3^- in floodwater were extremely low, however,
361 significantly more was NO_3^- observed in the dark-flood treatments (Fig. 3d). Across all
362 treatments, the loss of NO_3^- from the mesocosms was very low in the flooded treatments
363 ($<1.1 \text{ mg mesocosm}^{-1}$).

364 Overall, flooding induced both an increase in DON and DOC concentrations in soil
365 solution over time relative to the unflooded control (Fig. 4c). Concentrations tended to be
366 higher in the dark treatments. Once the floodwater had been removed, DOC concentrations
367 rapidly declined within 14 d, however, this decline was considerably slower for DON. Levels
368 of DOC in floodwater increased over time, however, the dynamics and treatment effect were
369 different to those seen in soil solution (Fig. 4d). In contrast, levels of DON in floodwater
370 remained low with few treatments effects apparent (Fig. 4b). The potential DON lost (mg
371 mesocosm^{-1}) was 28.3 ± 2.4 in T_1 , 27.5 ± 0.6 in T_2 and 14.7 ± 0.8 in T_4 and the potential
372 DOC lost (mg mesocosm^{-1}) was 362 ± 19 in T_1 , 352 ± 20 in T_2 and 339 ± 12 in T_4 .

373

374 3.2. Air quality: Greenhouse gas emissions

375 Figure 5 shows the daily production and cumulative fluxes of CH_4 , CO_2 and N_2O from
376 the last day of the flood stage and throughout the soil recovery stage. Daily CH_4 fluxes were
377 greatest at the end of flooding and rapidly declined after floodwater removal reaching fluxes
378 close to background 20 d after flood removal, especially for T_1 and T_2 (more constant for T_4 ,
379 flooding in the light). The highest cumulative CH_4 fluxes ($P = 0.003$) were found for
380 treatment including floods ($T_1 > T_2 > T_4 > T_5$; Fig. 5b). Daily CO_2 fluxes in the dark
381 treatments were initially higher than the illuminated treatments both at the end of the flood
382 stage and during soil recovery. This trend subsequently reversed after 2 weeks of soil
383 recovery. Although the dynamics of CO_2 production differed between treatments, the
384 cumulative amount of CO_2 produced over the recovery phase was similar (Fig. 5d). Daily

385 N₂O fluxes were highest in the darkened flood treatments (T₁ and T₂) and showed a
386 progressive production throughout the flood recovery stage (Fig. 5ef). When light was present
387 in the flood stage then almost no N₂O was produced, and responded in a near-identical way to
388 the unflooded control.

389

390 *3.3. Habitat provision and biological population regulation*

391 *3.3.1 Vegetation responses to extreme flooding*

392 As expected, the fertile agricultural Eutric Cambisol had a high base saturation, high
393 available P content, nitrification potential (NO₃⁻ > NH₄⁺; Table S1) and supported rapid
394 sward growth in the absence of flooding. After imposing the flood treatments and in the
395 absence of light, the vegetation was able to survive for approximately 3-4 weeks, however,
396 beyond this point, senescence and subsequent decomposition of the above-ground biomass
397 occurred (T₂ and T₃). Little recovery of this grass occurred in the subsequent recovery period
398 when the floodwater was removed and the soil allowed to dry out (Table 2). In contrast, when
399 light was present (T₄), a considerable amount of the above-ground vegetation was able to
400 survive throughout the flood period and readily recovered after floodwater removal. Despite
401 this sward recovery, grass production in the flooded treatments was less than produced in the
402 unflooded control (T₅).

403 No significant differences were observed for plant height, dry weight and mineral
404 nutrient concentration in the maize crop in the bioassay performed at the end of the
405 experiment (fourth phase). The only notable exceptions to this were the reduced growth for
406 plants grown in the T₁ [dark+flood (no veg.)] soil (SI, Table S2) and minimum alterations in
407 foliar C and K (SI, Table S3).

408

409

410 *3.3.2. Soil mesofauna*

411 Abundant earthworms were present in the soil at the start of the experiment. At the end
412 of the experiment, however, live earthworms could only be recovered from the soil of the
413 unflooded controls (Table 2).

414

415 3.3.3. Soil microbial biomass and community structure

416 Microbial PLFA analysis after the flood phase (Fig. 6a) and after soil recovery (Fig.
417 6b) showed that flooding induced a significant reduction in biomass relative to the unflooded
418 control. Microbial community structure was also significantly altered by flooding (Fig. 6cd).
419 Overall, flooding significantly decreased the amount of PLFAs indicative of protozoa ($P =$
420 0.014 and $P = 0.002$), putative arbuscular mycorrhizas ($P = 0.004$ and $P = 0.035$) and fungi (P
421 < 0.001 and $P < 0.001$), and increased the amount of Gram⁺ bacteria ($P < 0.001$ and $P =$
422 0.005) and actinomycetes ($P = 0.111$ and $P = 0.047$) in comparison with the unflooded control
423 (after flood and soil recovery stages, respectively, in each case). The PLFA ratios were also
424 altered by flooding, reducing fungi/bacteria ($P < 0.001$ and $P < 0.001$), predator/prey ($P =$
425 0.012 and $P = 0.001$) and 18w/19cyclo ($P = 0.043$ and $P = 0.020$) but increasing
426 Gram⁺/Gram⁻ ($P = 0.007$ and $P = 0.032$), sat/unsat ($P < 0.001$ and $P = 0.033$) and mono/poly
427 ($P < 0.001$ and $P = 0.002$) (Fig. 6ef).

428 Figure 7 shows the relationships in PLFA between the treatments after the flood and
429 soil recovery stages, i.e. taxonomic groups (Fig. 7ab) and fatty acids ratios (Fig. 7cd). These
430 PCAs show clear separation between the control and flood treatments with the absence of
431 light exacerbating the differences relative to the flooded treatment maintained in the light. At
432 the end of the flood stage, the first three components of the PCA (Fig. 7a) explained 75.2% of
433 the total variance. The first principal component (PC1) with a high loading for fungi, redox,
434 protozoa, Gram⁺ and NH₄⁺ accounted for 47.3%; the PC2 that explained 13% of the variance
435 (PC2) had a high loading for NO₃⁻ and N₂O. Some of the correlations of the variables used to
436 do the PCA were: fungi-redox ($r = 0.87$, $P < 0.001$), fungi-NH₄⁺ ($r = -0.89$, $P < 0.001$), fungi-

437 Gram+ ($r = -0.89$, $P < 0.001$), fungi-CH₄ ($r = -0.61$, $P = 0.006$), redox-Gram+ ($r = -0.89$, $P <$
438 0.001), and protozoa-Gram+ ($r = -0.86$, $P < 0.001$).

439 At the end of the soil recovery stage (Fig. 7b), PC1 had a high loading for Gram+,
440 actinomycetes (actino), fungi and anaerobic bacteria and explained 40% of the total variance
441 while PC2 explained 21.2%, with a high loading for Gram- bacteria followed by redox (79%
442 of total variance explained by the first 3 components). See Supp. Info for further information
443 relating to Fig. 7cd.

444 Table 3 shows the correlation matrix between GHG daily fluxes and soil parameters
445 during soil recovery stage. CH₄ emissions were related with anaerobic conditions (low redox
446 potential, high NH₄⁺ concentrations). Lastly, soil redox potential was negatively correlated to
447 NH₄⁺ in soil solution (Table 3).

448 Additional correlations between PLFAs and the most abundant fatty acids (> 2% of
449 the total PLFAs) and GHG daily fluxes, redox potential in soil, NH₄⁺ and NO₃⁻ are shown in
450 Table 4. CH₄ emissions were negatively correlated with PLFAs and the majority of these fatty
451 acids after the flood stage only. These negative correlations also occurred for NH₄⁺ after both
452 stages. CO₂ emission was negatively correlated with total PLFAs and many individual fatty
453 acids after the flooding stage but were positively related after the soil recovery stage (Table
454 4). As expected, redox potential in the soil was positively correlated with PLFAs in both
455 stages, indicating a higher microbial activity in the soil when redox potential is positive.

456

457 **4. Discussion**

458 This study clearly demonstrated that when soils with no previous history of flooding
459 are subjected to intense waterlogging, major changes in soil functions and ecosystem service
460 delivery occur. The simulated flood typologies reflect those seen recently in the UK and
461 elsewhere around the world (Dodds, 2014; Hai et al., 2017; Romshoo et al., 2018).

462 *4.1. Habitat provision: Primary productivity and earthworm abundance*

463 As expected, the vegetation in our mesocosms was heavily affected by long-term
464 flooding, especially when light was restricted (Mommer et al., 2005a, b; Das et al., 2009).
465 This suggests that alongside flood duration (Fig. S1-S4), the typology of the flood event is
466 also critical in determining the likelihood of vegetation survival. Extreme flooding can be
467 associated with large amounts of turbid sediment in the overlying water which restricts light
468 penetration (Fig. S3), whilst other flood events are associated with groundwater rise and
469 relatively clear overlying waters (Fig. S4). In recent years, extreme flood events in the UK
470 have been associated with large amounts of sediment in the floodwater which remains
471 suspended for long time periods via wind-mediated turbulence (Fig. S5). The impact of light
472 restriction and sediment load therefore requires greater consideration in future studies on the
473 impact of flooding on plant-soil systems (Squires et al., 2002). It is also clear from our study
474 that the presence of light favoured a more rapid recovery of grass production 5 weeks after
475 floodwater removal, however, no significant differences were observed in maize sown after
476 the soil recovery period in any treatment, highlighting the capacity of the soil to self-
477 ameliorate.

478 Earthworms perform vital functions in grasslands including the promotion of soil
479 organic matter turnover, nutrient recycling, aeration, drainage and the amelioration of
480 compaction (Langmaack et al., 1999). All of these attributes are frequently linked to greater
481 primary productivity. A decline in earthworm abundance, diversity or activity can therefore
482 be viewed as a severe loss of soil quality (Coyle et al., 2017). In our experiments, long-term
483 flooding resulted in a complete loss of the earthworm population with no recovery (i.e.
484 hatching from cocoons) observed 5 weeks after floodwater removal. This is in general
485 agreement with Ivask et al. (2012) who suggested that earthworm populations were
486 particularly affected by long term flooding. The loss of earthworms from all flooding
487 treatments in comparison with the unflooded controls could have potential short and long-
488 term effects on soil functionality (e.g. the loss of fertility, and a decline in soil structure).

489

490 4.2. *Impact of flooding on element cycling, water and air quality*

491 In our study, flooding increased soil pH, consistent with previous studies in rice paddy
492 soils and salt marshes by Ponnampereuma (1972) and Negrin et al. (2011), however, the
493 overall effect was small. We conclude that this is unlikely to cause lasting changes in nutrient
494 bioavailability or explain our flood-induced shifts in microbial diversity. A clear negative
495 effect of flooding on EC was apparent, however, the levels were insufficient to induce
496 osmotic stress in roots. We attribute the increase in EC to the release of mineral elements
497 from soil and during vegetation senescence (e.g. Fe, P, NH_4^+).

498 Flooding significantly altered the redox conditions in the soil, with all flood treatments
499 rapidly becoming anaerobic (Reddy and De Laune, 2008). However, the vegetation in T₄ kept
500 redox values higher than in T₁ and T₂ (without vegetation and in which vegetation died after
501 3-4 weeks of flood, respectively), probably because the plants were able to deliver oxygen to
502 the rhizosphere, alleviating the anaerobic conditions to some extent. Although this effect has
503 been observed for plant species such as *Spartina alterniflora* (Colmer, 2003), other authors
504 found no influence of vegetation on redox potential in soil with highly reduced conditions
505 (Negrin et al., 2011). This supports the tenet that selection of grass varieties with greater
506 potential for aerenchyma formation will offer greater protection against long term flooding
507 (de Souza et al., 2017).

508 The different element cycles (partially) assessed in this study were altered
509 considerably. There was a clear effect of flooding on Fe release (soil solution and floodwater),
510 however, a less clear pattern was apparent for P because the increase of P was only observed
511 in the floodwater of T₂ and T₃, treatments with vegetation and under light restrictions. We had
512 hypothesized that P held on the surface of Fe-oxyhydroxides would be released under
513 reducing conditions and would migrate upwards to the overlying floodwater where it might
514 stimulate algal production (Nanzyo et al., 2004; Heiberg et al., 2010), however, this was not

515 apparent. This could be due to any P released being reabsorbed back onto Al-hydroxides or
516 being immobilized by the microbial biomass. The evidence from the ^{33}P tracers also indicated
517 that the majority of solubilised P in the floodwater was actually derived from the
518 decomposing grass. Based on our field observations, it is also possible that Fe-P minerals may
519 have formed directly at the soil surface where the conditions are less anoxic (Lindsay et al.,
520 1989; Roden and Edmonds, 1997). The potential for P and Fe redistribution in soil during
521 flooding therefore warrants further research.

522 We ascribe the net accumulation of NH_4^+ during flooding to the mineralization of soil
523 organic matter (T_1), the necrosis of plant tissues and an inhibition of nitrification (Nielsen et
524 al., 1996). In the case of the soil, we cannot distinguish between N released from microbial
525 processes or from autolysis of live roots and subsequent excretion of NH_4^+ (Marella et al.,
526 2017). The low C:N ratio of earthworms (ca. 3:1) and vegetation (ca. 24:1) is likely to favour
527 net NH_4^+ release during their decomposition (Zheng and Marschner, 2017). In addition, when
528 photosynthesis is restricted and C for plant respiration becomes limited, root and shoot
529 autolysis will commence leading to NH_4^+ excretion to the external medium (i.e. during
530 proteolysis and creation of organic/keto acids; Marella et al., 2017). This operation of this
531 pathway is supported by the greater release of soluble N in treatments where light was
532 restricted. The NH_4^+ concentration in floodwater of T_2 during the flood stage was
533 approximately the sum of the concentrations of T_1 (soil without above-ground vegetation) and
534 T_3 (vegetation from T_1) treatments (Fig. 3b). This suggests that 35-40 % of the NH_4^+
535 originated from the above-ground vegetation and 60-65 % from the soil compartment.

536 In addition to plant uptake, losses of NH_4^+ via NH_3 volatilization (not determined in
537 this experiment) could also have occurred under inundation (Zhong-Cheng et al., 2012; Chen
538 et al., 2015). The high pH of the floodwater (pH 7.0-8.5) would favour this loss pathway and
539 could help explain the decrease in NH_4^+ for T_1 , T_2 and T_3 in the overlying water at the end of
540 the flood stage. During soil recovery, the soil water content of T_1 , T_2 and T_4 decreased,

541 resulting in re-aeration of the soil, re-establishment of nitrification, leading to a decrease in
542 NH_4^+ , and increases in NO_3^- and N_2O production.

543 Significant amounts of DOC and DON accumulated in the soil and overlying water
544 during flooding. This can be attributed to the release of organic compounds from organisms
545 killed by either (i) a lack of O_2 (e.g. mesofauna), (ii) osmotic shock, or (iii) metal toxicity
546 (e.g. by Fe^{2+} , Mn^{2+}) (Kieft et al., 1987, 1994; Deneff et al., 2001; Fierer and Schimel, 2003).
547 Based on the very high DOC-to-DON ratio (>70:1), however, we hypothesize that this C is
548 mainly derived from anaerobic respiration by-products (e.g. ethanol, organic acids) excreted
549 by plants and microbes into the external medium (Jones et al., 2009). Although soluble C
550 could also be released during the reduction and solubilisation of Fe-oxyhydroxides, this is not
551 favoured based on the DOC-to-DON ratio of soluble C held on the exchange surfaces of this
552 soil (ca. 12:1; Jones and Willett, 2006). The measured decrease in DOC concentration
553 following the removal of floodwater is most probably related to the removal of O_2 limitation
554 and a stimulation of microbial activity (Frank et al., 2014).

555 Although we used minimally disturbed blocks of vegetated soil in our mesocosms,
556 some aspects of real flood events could not be replicated. For example, in our experiment
557 there was no water turbulence and no erosional loss of soil, and the soil blocks were only 10
558 cm deep. While this reflects the main rooting zone, our results cannot be extrapolated easily
559 to subsoils where the C content and root density is much lower, and the effects of flooding
560 may be less severe. However, the nutrient losses due to the different flood typologies—
561 aggravated under light restriction—indicate the importance of considering the origin of the
562 floodwater, i.e. whether it contains suspended particles.

563 Alterations in the assessed gaseous emissions from the flooded mesocosms were also
564 dependent on flood typology. Normally, very low emissions of CO_2 , CH_4 and N_2O have been
565 observed during flooding in previous experiments with this soil (Sánchez-Rodríguez et al.,
566 2017). CH_4 emissions were, however, detected immediately after floodwater removal. We

567 ascribe this to the release of CH₄ produced during flooding, but which had become trapped
568 within the soil pores until floodwater removal (Moore and Roulet, 1993; Sánchez-Rodríguez
569 et al., 2017). In our experiment, the prevailing conditions under flooding (-100 mV redox
570 potential, high DOC, senescing vegetation) were ideal for CH₄ production (Hou et al., 2000).
571 This was most apparent in the dark treatments where plant senescence was greatest. As
572 oxygen was introduced back into the soil after flooding, and as alternative electron acceptors
573 became available (e.g. NO₃⁻), the rate of CH₄ emissions quickly decreased (Yuan et al.,
574 2008). This might also have been facilitated by an increase in CH₄ oxidation within the soil
575 (Zhang et al., 2012).

576 At the start of the soil recovery stage, the soil solution in the flooded treatments (T₁, T₂
577 especially, and T₄) had high concentrations of labile N and C (i.e. NH₄⁺, DON and DOC). In
578 addition, the soil redox potential increased, favouring conditions to produce N₂O (Hou et al.,
579 2000; Kim et al., 2010) as an intermediate product of nitrification. The observed decrease in
580 soil solution NO₃⁻ concentration during the soil recovery stage also indicates losses via
581 denitrification. However, the recovering vegetation under non-light restrictions could also
582 have acted as a NO₃⁻ sink, contributing to the daily and cumulative fluxes of N₂O, being
583 significantly lower for T₄ (flood+light) and T₅ or control in comparison with T₁ and T₂
584 (flood+dark without and with vegetation, respectively). Again, light restriction (flood
585 typology) and the presence of grass were essential to understand gaseous C and N losses.
586 Finally, it should be mentioned that, the limited depth of the mesocosms (10 cm) could have
587 underestimated the gas fluxes measured during the 5 weeks after the floodwater removal as
588 compared to field conditions but further research is needed to confirm this.

589

590 *4.3. Microbial biodiversity: Biological population regulation*

591 We present clear evidence that the microbial community was significantly affected by
592 prolonged flooding, the presence of vegetation and time since flooding. However, in some

593 flooding situations, water percolates through the soil in either an upward (groundwater
594 flooding) or downward (surface water flooding) direction. This mass flow may remove
595 microbial end-products and also change the redox status of the soil in comparison to our
596 mesocosms where no mass flow occurred.

597 Our results are in general agreement with Ferré et al. (2012) who found a higher
598 Gram+/Gram- bacteria ratio in flooded soils, probably as Gram+ bacteria (branched fatty
599 acids) are believed to be more stress tolerant than Gram- bacteria (monounsaturated fatty
600 acids). In addition, our results are in line with Reichardt et al. (2001) who found higher
601 concentrations of fungi in non-flooded conditions in comparison with flooded soils. In most
602 cases, however, the change in the individual amount of PLFAs was small in the different
603 treatments. However, it should be noted that this mainly reflects changes in the active
604 microbial biomass which may only represent <10% of the total PLFA in soil. The impact of
605 these changes in community structure on soil functioning remain uncertain due to the large
606 functional redundancy that exists in soil. What is clear, however, is that it had little impact on
607 plant growth and soil performance in our maize bioassay undertaken at the end of the
608 experiment. Further, in comparison to the loss of earthworms we expect that small shifts in
609 microbial community structure are of less importance in the longer term.

610 Other PLFA ratios were affected by the prolonged flooding treatments, for example
611 the ratio of sat/unsat agrees with the increase in saturated fatty acids under flooding described
612 in Bossio and Scow (1998), and 16w/17 cyclo and 18w/19 cyclo ratios that are related with
613 stress (Knivett and Cullen, 1965), probably due to low O₂ availability in the flooded
614 treatments. The detection of 16:1w7c and 18:1w9c fatty acids in soil taken at the end of the
615 flood period supports the presence of methanotrophs (Bedard and Knowles, 1989; Bowman et
616 al., 1991, 1993).

617 Lastly, the role of surviving vegetation in T₄ (flood+light, that facilitated less extreme
618 flood conditions) produced an intermediate PLFA profile between T₁-T₂ (flood under

619 darkness without and with soil, respectively) and T₅ (unflooded controls; Figs. 6, 7). The
620 oxygenation of the rhizosphere by living roots and a higher potential redox in T₄
621 (flood+light), probably lessened the impact of flooding and facilitated a quicker recovery of
622 the microbial community.

623

624 **5. Conclusions**

625 Prolonged flood events were shown to induce major shifts in the size and structure of
626 the soil microbial community that led to a decrease in air quality (higher net GHG emissions;
627 CH₄, N₂O) and major alterations in soil biogeochemical cycling as a function of the flood
628 typology. Prolonged flooding in which light is restricted increased the severity of the damage
629 in terms of potential nutrient losses, GHG emissions, soil microbial communities, grass
630 production and speed of recovery, highlighting the key role of the vegetation in maintaining
631 grassland soil functioning. We demonstrated that the decomposition of vegetation is an
632 important source of P loss, especially in flood typologies in which light is restricted where its
633 contribution can be as important as soil in terms of P loss rates. Our results also suggest that
634 anoxia-tolerant vegetation may play a key role in ameliorating the negative effects of flooding
635 on habitat provision, element cycling, and biological population regulation.

636

637 **Acknowledgments**

638 This work was supported by the Project ‘Legacy effects of the extreme flood events on
639 soil quality and ecosystem functioning’, NERC Grant Reference NE/M005143/1, by the UK
640 Department for Environment, Food and Rural Affairs (DEFRA) project LM0316, by the UK
641 Natural Environment Research Council (NE/I012303/1) and the Sêr Cymru LCEE-NRN
642 project, Climate-Smart Grass. Sánchez-Rodríguez also acknowledges funding support by the
643 ‘Fundación Ramón Areces’ for his postdoctoral scholarship “Beca para ampliación de
644 estudios en el extranjero en materia de Ciencias de la Vida y de la Materia”.

645

646

647

648 **References**

649 Adrian, W.J., 1973. A comparison of a wet pressure digestion method with other commonly
650 used wet and dry-ashing methods. *Analyst* 98, 213–216.

651 Allan, R.P., 2011. Human influence on rainfall. *Nature* 470, 344–345.

652 Bartelt-Ryser, J., Joshi, J., Schmid, B., Brandl, H., Balsler, T., 2005. Soil feedbacks of plant
653 diversity on soil microbial communities and subsequent plant growth. *Perspectives in*
654 *Plant Ecology, Evolution and Systematics* 7, 27–49.

655 Bedard, C., Knowles, R., 1989. Physiology, biochemistry, and specific inhibitors of CH₄,
656 NH₄⁺, and CO oxidation by methanotrophs and nitrifiers. *Microbiology Reviews* 53,
657 68–84.

658 Bossio, D.A., Scow, K.M., 1998. Impacts of carbon and flooding on soil microbial
659 communities: phospholipid fatty acid profiles and substrate utilization patterns.
660 *Microbial Ecology* 35, 265–278.

661 Bowman, J.P., Skerratt, J.H., Nichols, P.D., Sly, L.I., 1991. Phospholipid fatty-acid and
662 lipopolysaccharide fatty-acid signature lipids in methane-utilizing bacteria. *FEMS*
663 *Microbiology Ecology* 85, 15–22.

664 Bowman, J.P., Sly, L.I., Nichols, P.D., Hayward, A.C., 1993. Revised taxonomy of the
665 methanotrophs - description of *Methylobacter* gen-nov, emendation of *Methylococcus*,
666 validation of *Methylosinus* and *Methylocystis* species, and a proposal that the family
667 *Methylococcaceae* includes only the group-I methanotrophs. *International Journal of*
668 *Systematic Bacteriology* 43, 735–753.

669 Brun, J., Barros, A.P., 2013. Vegetation activity monitoring as an indicator of eco-
670 hydrological impacts of extreme events in the southeastern USA. *International Journal*
671 *of Remote Sensing* 34, 519–544.

672 Bünemann, E.K., Bongiorno, G., Bai, Z., Creamer, R.E., de Deyn, G., de Goede R., Fleskens,
673 L., Geissen, V., Kuyper, T.W., Mäder, P., Pulleman, M., Sukkel, W., van Groenigen,
674 J.W., Brussaard, L., 2018. Soil quality – A critical review. *Soil Biology and*
675 *Biochemistry* 120, 105–125.

676 Chen, A., Lei, B., Hu, W., Lu, Y., Mao, Y., Duan, Z., Shi, Z., 2015. Characteristics of
677 ammonia volatilization on rice grown under different nitrogen application rates and its
678 quantitative predictions in Erhai Lake Watershed, China. *Nutrient Cycling in*
679 *Agroecosystems* 101, 139–152.

680 Clout, H., 2014. Reflections on the draining of the Somerset Levels. *The Geographical*
681 *Journal* 180, 338–341.

682 Colmer, T.D., 2003. Long-distance transport of gases in plants: a perspective on internal
683 aeration and radial oxygen loss from roots. *Plant Cell and Environment* 26, 17–36.

684 Coyle, D.R., Nagendra, U.J., Taylor, M.K., Campbell, J.H., Cunard, C.E., Joslin, A.H.,
685 Mundepi, A., Phillips, C.A., Callahan, M.A., 2017. Soil fauna responses to natural
686 disturbances, invasive species, and global climate change: Current state of the science
687 and a call to action. *Soil Biology and Biochemistry* 110, 116–133.

688 Das, K.K., Panda, D., Sarkar, R.K., Reddy, J.N., Ismail, A.M., 2009. Submergence tolerance
689 in relation to variable floodwater conditions in rice. *Environmental and Experimental*
690 *Botany* 66, 425–434.

691 de Souza, K.R.D., Santos, M.D., Andrade, C.A., da Silva, D.M., Campos, N.A., Alves, J.D.,
692 2017. Aerenchyma formation in the initial development of maize roots under
693 waterlogging. *Theoretical and Experimental Plant Physiology* 29, 165–175.

694 Deneff, K.J., Six, J., Bossuyt, H., Frey, S.D., Elliot, E.T., Merckx, R., Paustian, K., 2001.
695 Influence of dry-wet cycles on the interrelationship between aggregate, particulate
696 organic matter, and microbial community dynamics. *Soil Biology and Biochemistry* 33,
697 1599–1611.

698 Dodds, K., 2014. Apres le deluge: the UK winter storms of 2013-14. *Geographical Journal*
699 180, 294–296.

700 Doran, J.W., Parkin, T.B., 1994. Defining and assessing soil quality. In: Doran, J.W.,
701 Coleman, D.C., Bezdicek, D.F., Stewart, B.A. (Eds.), *Defining Soil Quality for a*
702 *Sustainable Environment*. SSSA, Madison, WI, pp. 3–21.

703 Doran, J.W., Parkin, T.B., 1996. Quantitative indicators of soil quality: a minimum data set.
704 In: Doran, J.W., Jones, A.J. (Eds.), *Methods for Assessing Soil Quality*. Soil Science
705 Society of America, Madison, WI, pp. 25–37.

706 Easterling, D.R., Meehl, G.A., Parmesan, C., Changnon, S.A., Karl, T.R., Mearns, L.O., 2000.
707 Climate extremes: Observations, modeling, and impacts. *Science* 289, 2068–2074.

708 Ferré, C., Zechmeister-Boltenstern, S., Comolli, R., Andersson, M., Seufert, G., 2012. Soil
709 microbial community structure in a rice paddy field and its relationships to CH₄ and
710 N₂O fluxes. *Nutrient Cycling in Agroecosystems* 93, 35–50.

711 Fierer, N., Schimel, J.P., 2003. A proposed mechanism for the pulse in carbon dioxide
712 production commonly observed following the rapid rewetting of a dry soil. *Soil Science*
713 *Society of America Journal* 67, 798–805.

714 Frank, S., Tiemeyer, B., Gelbrecht, J., Freibauer, A., 2014. High soil solution carbon and
715 nitrogen concentrations in a drained Atlantic bog are reduced to natural levels by 10
716 years of rewetting. *Biogeosciences* 11, 2309–2324.

717 Frostegård, Å, Tunlio, A., Bååth, E., 2011. Use and misuse of PLFA measurements in soils.
718 *Soil Biology and Biochemistry* 43, 1621–1625.

719 Frostegård, Å., Bååth, E., Tunlid, A., 1993. Shifts in the structure of soil microbial
720 communities in limed forests as revealed by phospholipid fatty acid analysis. *Soil*
721 *Biology and Biochemistry* 25, 723–730.

722 Giesler, R., Lundström, U.S., 1993. Soil solution chemistry: The effects of bulking soil
723 samples and spatial variation. *Soil Science Society of America Journal* 57, 1283–1288.

724 Hai, O.S., Abu Samah, A., Chenoli, S.N., Subramaniam, K., Mazuki, M.Y.A., 2017. Extreme
725 Rainstorms that Caused Devastating Flooding across the East Coast of Peninsular
726 Malaysia during November and December 2014. *Weather and Forecasting* 32, 49–872.

727 Heiberg, L., Pedersen, T.V., Jensen, H.S., Kjaergaard, C., Hansen, H.C.B., 2010. A
728 comparative study of phosphate sorption in lowland soils under oxic conditions. *Journal*
729 *of Environmental Quality* 39, 734–743.

730 Hou, A.X., hen, G.X., Wang, Z.P., Van Cleemput, O., Patrick Jr., W.H., 2000. Methane and
731 nitrous oxide emissions from a rice field in relation to soil redox and microbiological
732 processes. *Soil Science Society of America Journal* 64, 2180–2186.

733 Ivask, M., Meriste, M., Kuu, A., Kutti, S., Sizov, E., 2012. Effect of flooding by fresh and
734 brackish water on earthworm communities along Matsalu Bay and the Kasari River.
735 *European Journal of Soil Biology* 53, 11–15.

736 Jones, D.L., Nguyen, C., Finlay, R.D., 2009. Carbon flow in the rhizosphere: carbon trading
737 at the soil-root interface. *Plant and Soil* 321, 5–33.

738 Jones, D.L., Willett, V.B., 2006. Experimental evaluation of methods to quantify dissolved
739 organic nitrogen (DON) and dissolved organic carbon (DOC) in soil. *Soil Biology and*
740 *Biochemistry* 38, 991–999.

741 Jones, M.R., Fowler, H.J., Kilsby, C.G., Blenkinsop, S., 2012. An assessment of changes in
742 seasonal and annual extreme rainfall in the UK between 1961 and 2009. *International*
743 *Journal of Climatology* 33, 1178–1194.

744 Kieft, T.E., Soroker, E., Firestone, M.K., 1987. Microbial biomass response to a rapid
745 increase in water potential when dry soil is wetted. *Soil Biology & Biochemistry* 19,
746 119–126.

747 Kieft, T.L., Ringelberg, D.B., White, D.C., 1994. Changes in ester linked phospholipid fatty
748 acid profiles of subsurface bacteria during starvation and desiccation in a porous
749 medium. *Applied and Environmental Microbiology* 60, 3292–3299.

750 Kim, D.G., Mishurov, M., Kiely, G., 2010. Effect of increased N use and dry periods on N₂O
751 emission from fertilized grasslands. *Nutrient Cycling in Agroecosystems* 88, 397-410.

752 Knivett, V.A., Cullen, J., 1965. Some factors affecting cyclopropane acid formation in
753 *Escherichia coli*. *Biochemical Journal* 96, 771–776.

754 Langmaack, M., Schrader, S., Rapp-Bernhardt, U., Kotzke, K., 1999. Quantitative analysis of
755 earthworm burrow systems with respect to biological soil-structure regeneration after
756 soil compaction. *Biology and Fertility of Soils* 28, 219–229.

757 Lindsay, W.L., Vlek, P.L.G., Chien, S.H., 1989. Phosphate minerals. In: Dixon, J.B., Weed,
758 S.B. (Eds.), *Minerals in soil environments*. Soil Science Society of America, Madison,
759 WI, pp. 1089–1130.

760 Loeppert, R.H., Inskeep, W.P., 1996. Iron. In: Sparks, D.L. (Ed.), *Methods of Soil Analysis*.
761 Part 3. Chemical Methods. ASA/SSSA, Madison, pp. 639–664.

762 MacKenzie, A.F., Fan, M.S., Cadrin, F., 1998. Nitrous oxide emission in three years as
763 affected by tillage, corn-soybean-alfalfa rotations, and nitrogen fertilization. *Journal of*
764 *Environmental Quality* 27, 698–703.

765 Marella, V.S.S.R., Roberts, P., Hill, P.W., Jones, D.L., 2017. Different ways in which CO₂
766 can be released during the turnover of roots in soil. *Biology and Fertility of Soils* 53,
767 369–374.

768 McEwen, L.J., Jones, O., Robertson, I., 2014. ‘A glorious time?’ Some reflections on flooding
769 in the Somerset Levels. *Geographical Journal* 180, 326–337.

770 Met Office - United Kingdom, 2014. The Recent Storms and Floods in the UK. Available
771 at:<http://www.http://nora.nerc.ac.uk/id/eprint/505192/1/N505192CR.pdf> (10th June
772 2018)

773 Miranda, K.M, Espey, M.G., Wink, D.A., 2001. A rapid simple spectrophotometric method
774 for simultaneous detection of nitrate and nitrite. *Nitric Oxide: Biology and Chemistry* 5,
775 62–71.

776 Mommer, L., de Kroon, H., Pierik, R., Bogemann, G.M., Visser, E.J.W., 2005b. A functional
777 comparison of acclimation to shade and submergence in two terrestrial plant species.
778 *New Phytologist* 167, 197–206.

779 Mommer, L., Pons, T.L., Wolters-Arts, M., Venema, J.H., Visser, E.J.W., 2005a.
780 Submergence-induced morphological, anatomical, and biochemical responses in a
781 terrestrial species affect gas diffusion resistance and photosynthetic performance. *Plant*
782 *Physiology* 139, 497–508.

783 Moore, T.R., Roulet, N.T., 1993. Methane flux - water-table relations in northern wetlands.
784 *Geophysical Research Letters* 20, 587–590.

785 Mulvaney, R.L., 1996. Nitrogen - inorganic forms. In: Sparks, D.L. (Ed.), *Methods of Soil*
786 *Analysis. Part 3. Chemical Methods*. Soil Science Society of America, Madison, WI,
787 pp. 1123–1184.

788 Murphy, J., Riley, J.P., 1962. A modified single solution method for the determination of
789 phosphate in natural waters. *Analytica Chimica Acta* 27, 31–36.

790 Murphy, J.M., Sexton, D.M.H., Jenkins, G.J., Boorman, P., Booth, B., Brown, K., Clark, R.,
791 Collins, M., Harris, G., Kendon, L., 2009. UK climate projections science report:
792 Climate change projections. Met Office Hadley Centre, Exeter, UK.

793 Nanzyo, M., Kanno, H., Obara, S., 2004. Effect of reducing conditions on P sorption of soils.
794 *Soil Science and Plant Nutrition* 50, 1023–1028.

795 Natural England, 2014. An assessment of the effects of the 2013-14 flooding on the wildlife
796 and habitats of the Somerset levels and moors: Report JP007. Natural England,
797 Worcester.

798 Negrin, V.L., Spetter, C.V., Asteasuain, R.O., Perillo, G.M.E., Marcovecchio, J.E., 2011.
799 Influence of flooding and vegetation on carbon, nitrogen, and phosphorus dynamics in
800 the pore water of a *Spartina alterniflora* salt marsh. Journal of Environmental Science
801 23, 212–221.

802 Nelson, R.E., 1982. Carbonate and gypsum. In: Page, A.L. (Ed.), Methods of Soil Analysis.
803 Part 2. Chemical and Microbiological Properties. Soil Science Society of America,
804 Madison, WI, pp. 181–197.

805 Nielsen, T.H., Nielsen, L.P., Revsbech, N.P., 1996. Nitrification and coupled nitrification-
806 denitrification associated with a soil-manure interface. Soil Science Society of America
807 Journal 60, 1829–1840.

808 Niklaus, P.A., Alpehi, J., Ebersberger, D., Kampichler, D., Kandeler, E., Tscherko, D., 2003.
809 Six years of in situ CO₂ enrichment evoke changes in soil structure and soil biota of
810 nutrient-poor grassland. Global Change Biology 9, 585–600.

811 Niu, S., Luo, Y., Li, D., Cao, S., Xia, J., Li, J., Smith, M.D., 2014. Plant growth and mortality
812 under climatic extremes: An overview. Environmental and Experimental Botany 98,
813 13–19.

814 Norton, J.M., 2008. Nitrification in agricultural soils, in: Schepers, J.S., Raun, W.R. (Eds.),
815 Nitrogen in Agricultural Systems. Agron. Monogr. 49. American Society of Agronomy,
816 Crop Science Society of America, Soil Science Society of America, Madison, WI, (Ch.
817 6), pp. 173–199.

818 Olsson, P.A., Thingstrup, I., Jakobsen, I., Baath, F., 1999. Estimation of the biomass of
819 arbuscular mycorrhizal fungi in a linseed field. Soil Biology and Biochemistry 31,
820 1879–1887.

821 Pall, P., Aina, T., Stone, D.A., Stott, P.A., Nozawa, T., Hilberts, A.G.J., Lohmann, D., Allen,
822 M.R., 2011. Anthropogenic greenhouse gas contribution to flood risk in England and
823 Wales in autumn 2000. *Nature* 470, 382–385.

824 Palomo, L., Claaseen, N., Jones, D.L., 2006. Differential mobilization of P in the maize
825 rhizosphere by citric acid and potassium citrate. *Soil Biology and Biochemistry* 38,
826 683–692.

827 Paul, E.A., Clark, F.E., 1996. *Soil Microbiology and Biochemistry*. Academic Press, San
828 Diego, CA.

829 Ponnampereuma, F.N., 1972. *The Chemistry of Submerged Soils*. Academic Press, New York.

830 Ratledge, C., Wilkinson, S.G., 1988. *Microbial Lipids*. Academic Press, London.

831 Reddy, K.R., De Laune, R.D., 2008. *Biogeochemistry of wetlands: science and applications*.
832 CRC Press, Boca Raton, FL.

833 Reichardt, W., Briones, A., de Jesus, R., Padre, B., 2001. Microbial population shifts in
834 experimental rice systems. *Applied Soil Ecology* 17, 151–163.

835 Roden, E.E., Edmonds, J.W., 1997. Phosphate mobilization in iron-rich anaerobic sediments:
836 microbial Fe (III) oxide reductions versus iron-sulphide formation. *Archives of*
837 *Hydrobiology* 139, 347–378.

838 Romshoo, S.A., Altaf, S., Rashid, I., Dar, R.A., 2018. Climatic, geomorphic and
839 anthropogenic drivers of the 2014 extreme flooding in the Jhelum basin of Kashmir,
840 India. *Geomatics Natural Hazards & Risk* 9, 224–248.

841 Sánchez-Rodríguez, A.R., Chadwick, D.R., Tatton, G.S., Hill, P.W., Jones, D.L., 2018.
842 Comparative effects of prolonged freshwater and saline flooding on nitrogen cycling in
843 an agricultural soil. *Applied Soil Ecology* 125, 56–70
844 <https://doi.org/10.1016/j.apsoil.2017.11.022>.

845 Sánchez-Rodríguez, A.R., Hill, P.W., Chadwick, D.R., Jones, D.L., 2017. Crop residues
846 exacerbate the negative effects of extreme flooding on soil quality. *Biology and Fertility*
847 *of Soils* 53, 751–765

848 Scalenghe, R., Edwards, A.C., Barberis, E., 2007. Phosphorus loss in overfertilized soils: the
849 selective P partitioning and redistribution between particle size separates. *European*
850 *Journal of Agronomy* 27, 72–80.

851 Scalenghe, R., Edwards, A.C., Barberis, E., Ajmone-Marsan, F., 2012. Are agricultural soils
852 under a continental temperate climate susceptible to episodic reducing conditions and
853 increased leaching of phosphorus? *Journal of Environmental Management* 97, 141–147.

854 Shaw, R.E., Meyers, W.S., McNeill, A., Tyerman, S.D., 2013. Waterlogging in Australian
855 agricultural landscapes: a review of plant response and crop models. *Crop and Pasture*
856 *Science* 64, 549–562.

857 Smith, J.L., Doran, J.W., 1996. Measurement and use of pH and electrical conductivity for
858 soil quality analysis. *Methods for Assessing Soil Quality*. SSSA Special Publication 49.
859 Soil Science Society of America, Madison, WI, pp. 169–185.

860 Squires, M.M., Lesack, L.F.W., Huebert, D., 2002. The influence of water transparency on
861 the distribution and abundance of macrophytes among lakes of the Mackenzie Delta,
862 Western Canadian Arctic. *Freshwater Biology* 47, 2123–2135.

863 Thorne, C., 2014. Geographies of UK Flooding in 2013/4. *Geographical Journal* 180, 297–
864 309.

865 Yuan, W.L., Cao, C.G., Cheng, J.P., Xie, N.N., 2008. CH₄ and N₂O emissions and their
866 GWPs assessment in intermittent irrigation rice paddy field. *Scientia Agricultura Sinica*
867 41, 4294–4300.

868 Zelles, L., 1999. Fatty acids patterns of phospholipids and lipopolysaccharides in the
869 characterization of microbial communities in soil: a review. *Biology and Fertility of*
870 *Soils* 29, 111–129.

871 Zhang, G.B., Ji, Y., Ma, J., Xu, H., Cai, Z.C., Yagi, K., 2012. Intermittent irrigation changes
872 production, oxidation, and emission of CH₄ in paddy fields determined with stable
873 carbon isotope technique. *Soil Biology and Biochemistry* 52, 108–116.

874 Zheng, B., Marschner, P., 2017. Previous residue addition rate and C/N ratio influence
875 nutrient availability and respiration rate after the second residue addition. *Geoderma*
876 285, 217–224.

877 Zhong-Cheng, L., Qi-Gen, D., Shi-Chao, Y., Fu-Guan, W., Yu-Shu, J., Jing-Dou, C., Lu-
878 Shen, X., Hong-Cheng, Z., Zhong-Yang, H., Ke, X., Hai.Yan, W., 2012. Effects of
879 nitrogen application levels on ammonia volatilization and nitrogen utilization during
880 rice season. *Rice Science* 19, 125–134.

881

882

883

884

885

886

887

888

889

890

891

892

893

894

895

896

897
898
899
900
901
902
903
904
905
906
907
908
909
910
911
912
913
914
915
916
917
918
919
920
921

Figure legends

Fig. 1 Time course (mean value) of pH and EC in soil solution and flood water, and redox potential in soil, as a function of flood treatments. Vertical bars in the upper part represent Bonferroni values at $\alpha = 0.05$ and the presence of asterisk/s indicate significant differences (*: $P < 0.05$, **: $P < 0.01$, ***: $P < 0.001$). T1: soil samples without vegetation, flooded and kept under darkness. T2: soil samples with vegetation, flooded and kept under darkness. T3: vegetation cut from T1 before the flood stage, flooded and under kept under darkness. T4: soil samples with vegetation, flooded and maintained in the light. T5 (control): soil samples with vegetation and maintained in the light. Four replicates per treatment.

Fig. 2 Time course (mean value) of Fe, P and ^{33}P in soil solution and flood water as a function of flood treatments. Vertical bars in the upper part represent Bonferroni values at $\alpha = 0.05$ and the presence of asterisk/s indicate significant differences (*: $P < 0.05$, **: $P < 0.01$, ***: $P < 0.001$). T1: soil samples without vegetation, flooded and kept under darkness. T2: soil samples with vegetation, flooded and kept under darkness. T3: vegetation cut from T1 before the flood stage, flooded and under kept under darkness. T4: soil samples with vegetation, flooded and maintained in the light. T5 (control): soil samples with vegetation and maintained in the light. Four replicates per treatment.

922 **Fig. 3** Time course (mean value) of NH_4^+ and NO_3^- in soil solution and flood water as a
923 function of flood treatments. Vertical bars in the upper part represent Bonferroni values at $\alpha =$
924 0.05 and the presence of asterisk/s indicate significant differences (*: $P < 0.05$, **: $P < 0.01$,
925 ***: $P < 0.001$). T1: soil samples without vegetation, flooded and kept under darkness. T2:
926 soil samples with vegetation, flooded and kept under darkness. T3: vegetation cut from T1
927 before the flood stage, flooded and under kept under darkness. T4: soil samples with
928 vegetation, flooded and maintained in the light. T5 (control): soil samples with vegetation and
929 maintained in the light. Four replicates per treatment.

930

931 **Fig. 4** Time course (mean value) of DON and DOC in soil solution and flood water as a
932 function of flood treatments. Vertical bars in the upper part represent Bonferroni values at $\alpha =$
933 0.05 and the presence of asterisk/s indicate significant differences (*: $P < 0.05$, **: $P < 0.01$,
934 ***: $P < 0.001$). T1: soil samples without vegetation, flooded and kept under darkness. T2:
935 soil samples with vegetation, flooded and kept under darkness. T3: vegetation cut from T1
936 before the flood stage, flooded and under kept under darkness. T4: soil samples with
937 vegetation, flooded and maintained in the light. T5 (control): soil samples with vegetation and
938 maintained in the light. Four replicates per treatment.

939

940 **Fig. 5** Daily (left) and cumulative (right) fluxes of CH_4 , CO_2 and N_2O (mean value) during
941 the soil recovery stage as a function of flood treatments. Different letters mean differences
942 according to Bonferroni multiple comparison test for daily fluxes and Tukey's HSD test for
943 the last determination of cumulative fluxes at a probability level of 0.05. Vertical bars in the
944 upper part represent Bonferroni and Tukey's HSD values, respectively for daily and
945 cumulative fluxes, at $\alpha = 0.05$ and the presence of asterisk/s indicate significant differences
946 (*: $P < 0.05$, **: $P < 0.01$, ***: $P < 0.001$). T1: soil samples without vegetation, flooded and
947 kept under darkness. T2: soil samples with vegetation, flooded and kept under darkness. T4:

948 soil samples with vegetation, flooded and maintained in the light. T5 (control): soil samples
949 with vegetation and maintained in the light. Four replicates per treatment.

950

951 **Fig. 6** Total amount of PLFAs from soil samples (a, b), taxonomic groups (c, d) and ratios (e ,
952 f) based on PLFAs after flood stage (left) and after soil recovery stage (right) as a function of
953 flood treatments. Different letters mean differences according to Tukey's HSD test at a
954 probability level of 0.05. T1: soil samples without vegetation, flooded and kept under
955 darkness. T2: soil samples with vegetation, flooded and kept under darkness. T4: soil samples
956 with vegetation, flooded and maintained in the light. T5 (control): soil samples with
957 vegetation and maintained in the light. Four replicates per treatment.

958

959 **Fig. 7** Principal component analysis for PLFAs (taxonomic groups and ratios based on
960 PLFAs), GHG emissions, redox potential in soil, NH_4^+ and NO_3^- in soil solution after flood
961 stage (a and c) and after soil recovery stage (b and d) as a function of flood treatments. The
962 separation between treatments or biplot is shown at the left and the corresponding loading of
963 each variable included in the PCA at right. T1: soil samples without vegetation, flooded and
964 kept under darkness. T2: soil samples with vegetation, flooded and kept under darkness. T3:
965 vegetation cut from T1 before the flood stage, flooded and under kept under darkness. T4: soil
966 samples with vegetation, flooded and maintained in the light. T5 (control): soil samples with
967 vegetation and maintained in the light. Four replicates per treatment.

Table 1

Fatty acids considered in the study to establish the different taxonomic groups whose concentration is greater than 0.5% of the total PLFAs.

Taxonomic group	Fatty acid	References
Gram+ bacteria	14:0 iso, 15:0 iso, 15:0 anteiso, 15:1 iso w6c, 16:0 iso, 17:0 iso, 17:0 anteiso, 17:1 iso w9c	Ratledge and Wilkinson (1988), Kieft et al. (1994), Paul and Clark (1996), Zelles (1999), Olsson et al. (1999), Bartelt-Ryser et al. (2005)
Gram- bacteria	16:1w7c, 16:1w9c, 17:1w8c, 17:0 cyclo w7c, 18:1w5c, 18:1w7c, 18:1w9c, 19:0 cyclo w7c	Bedard and Knowles (1989), Bossio and Scow (1998), Bowman et al. (1991, 1993), Kieft et al. (1994), Paul and Clark (1996), Zelles (1999)
Actinomycetes	16:0 10 methyl, 18:0 10 methyl, 10 methyl 19:1 w7c	Zelles (1999)
Anaerobic bacteria	15:0 dma	
Protozoa	20:4w6	Paul and Clark (1996)
Fungi	18:2w6	Paul and Clark (1996)
Putative arbuscular mycorrhiza	16:1w5c	Olsson et al. (1999)
Not assigned	14:0, 15:0, 16:0, 17:0, 18:0	Ratledge and Wilkinson (1988), Niklaus et al. (2003)

Table 2

Grass above-ground dry weight and number of earthworms at the end of the soil recovery stage as a function of the flooding treatment. *P* is the ANOVA *P*-value. Different letters indicate differences between treatments according to Tukey's HSD *post hoc* test ($P < 0.05$). Four replicates per treatment.

Treatment	Grass production (g mesocosm ⁻¹)	Earthworms (mesocosm ⁻¹)
T ₁ : Flood + dark (no veg)	0.5 ± 0.1 c	0.0 ± 0.0 b
T ₂ : Flood + dark	0.6 ± 0.1 c	0.0 ± 0.0 b
T ₄ : Flood + light	10.9 ± 2.2 b	0.0 ± 0.0 b
T ₅ : Control + light	28.0 ± 1.8 a	4.8 ± 0.8 a
<i>P</i>	< 0.001	< 0.001

T₁: Flood + dark (no veg.): soil samples without vegetation, flooded and maintained in the dark.
T₂: Flood + dark: soil samples with vegetation, flooded and maintained in the dark.
T₄: Flood + light: soil samples with vegetation, flooded and maintained in the light.
T₅: Control + light: soil samples with vegetation, no flooding and maintained in the light.

Table 4 | Correlation matrix showing the relationship between microbially-derived phospholipid fatty acids (which constitute >2 % total of PLFAs) and soil quality parameters (greenhouse gas daily fluxes, redox potential in soil, NH_4^+ and NO_3^- in soil solution) for soils directly after flooding and after a further 5 week recovery phase.

PLFA	15:0 iso	15:0 anteiso	16:0 iso	16:1 w7c	16:1 w5c	16:0	16:0 methyl	17:0 cyclo w7c	18:2 w6c	18:1 w9c	18:1 w7c	18:0	18:0 methyl	19:0 cyclo w7c
After the removal of flooding														
CH_4	-0.62 $P=0.010$	-0.44 $P=0.085$	-0.45 $P=0.081$	-0.61 $P=0.013$	-0.57 $P=0.022$	-0.60 $P=0.015$	-0.69 $P=0.003$	-0.61 $P=0.012$	-0.58 $P=0.018$	-0.59 $P=0.016$	-0.58 $P=0.018$	-0.51 $P=0.043$	-0.29 $P=0.281$	-0.54 $P=0.032$
CO_2	-0.60 $P=0.016$	-0.17 $P=0.525$	-0.31 $P=0.239$	-0.55 $P=0.028$	-0.50 $P=0.047$	-0.62 $P=0.011$	-0.51 $P=0.045$	-0.55 $P=0.026$	-0.77 $P<0.001$	-0.62 $P=0.010$	-0.60 $P=0.013$	-0.53 $P=0.036$	-0.20 $P=0.460$	-0.35 $P=0.187$
N_2O	-0.08 $P=0.763$	-0.112 $P=0.682$	-0.188 $P=0.487$	0.03 $P=0.907$	-0.03 $P=0.911$	-0.09 $P=0.754$	-0.04 $P=0.888$	-0.08 $P=0.776$	0.03 $P=0.890$	-0.14 $P=0.609$	-0.09 $P=0.728$	-0.15 $P=0.572$	-0.322 $P=0.224$	-0.20 $P=0.463$
Redox	0.55 $P=0.026$	0.32 $P=0.877$	0.25 $P=0.349$	0.51 $P=0.043$	0.66 $P=0.006$	0.47 $P=0.067$	0.69 $P=0.003$	0.66 $P=0.005$	0.82 $P<0.001$	0.57 $P=0.022$	0.56 $P=0.024$	0.49 $P=0.053$	0.28 $P=0.290$	0.39 $P=0.134$
NH_4^+	-0.78 $P<0.001$	-0.40 $P=0.126$	-0.50 $P=0.049$	-0.77 $P<0.001$	-0.78 $P<0.001$	-0.77 $P<0.001$	-0.77 $P<0.001$	-0.81 $P<0.001$	-0.85 $P<0.001$	-0.74 $P<0.001$	-0.80 $P<0.001$	-0.70 $P=0.002$	-0.32 $P=0.222$	-0.54 $P=0.029$
NO_3^-	-0.22 $P=0.410$	0.12 $P=0.670$	-0.17 $P=0.54$	-0.13 $P=0.629$	-0.17 $P=0.528$	-0.21 $P=0.445$	-0.23 $P=0.392$	-0.22 $P=0.414$	-0.34 $P=0.192$	-0.31 $P=0.244$	-0.24 $P=0.372$	-0.22 $P=0.403$	-0.27 $P=0.310$	-0.25 $P=0.351$
After soil recovery														
CH_4	0.18 $P=0.495$	0.16 $P=0.551$	0.09 $P=0.734$	0.22 $P=0.402$	0.03 $P=0.926$	0.23 $P=0.383$	0.11 $P=0.693$	0.07 $P=0.793$	0.18 $P=0.513$	0.18 $P=0.513$	0.19 $P=0.492$	0.08 $P=0.758$	-0.02 $P=0.945$	0.14 $P=0.600$
CO_2	0.59 $P=0.016$	0.29 $P=0.282$	0.43 $P=0.098$	0.46 $P=0.071$	0.45 $P=0.078$	0.62 $P=0.011$	0.56 $P=0.026$	0.59 $P=0.016$	0.64 $P=0.007$	0.54 $P=0.030$	0.59 $P=0.016$	0.41 $P=0.119$	0.29 $P=0.271$	0.56 $P=0.024$
N_2O	-0.25 $P=0.350$	0.07 $P=0.808$	-0.15 $P=0.570$	-0.26 $P=0.340$	-0.28 $P=0.293$	-0.25 $P=0.352$	-0.05 $P=0.841$	-0.21 $P=0.424$	-0.31 $P=0.236$	-0.23 $P=0.390$	-0.25 $P=0.352$	-0.35 $P=0.190$	-0.25 $P=0.346$	-0.13 $P=0.637$
Redox	0.48 $P=0.058$	0.27 $P=0.318$	0.48 $P=0.063$	0.35 $P=0.191$	0.54 $P=0.033$	0.43 $P=0.098$	0.44 $P=0.092$	0.55 $P=0.026$	0.52 $P=0.038$	0.44 $P=0.087$	0.43 $P=0.095$	0.54 $P=0.031$	0.60 $P=0.015$	0.60 $P=0.013$
NH_4^+	-0.71 $P=0.002$	0.48 $P=0.064$	-0.54 $P=0.029$	-0.62 $P=0.011$	-0.64 $P=0.007$	-0.71 $P=0.002$	-0.57 $P=0.022$	-0.71 $P=0.002$	-0.73 $P=0.001$	-0.67 $P=0.001$	-0.69 $P=0.003$	-0.61 $P=0.011$	-0.46 $P=0.070$	-0.57 $P=0.020$
NO_3^-	-0.15 $P=0.570$	0.19 $P=0.486$	0.04 $P=0.890$	0.20 $P=0.448$	0.00 $P=0.990$	0.20 $P=0.456$	0.06 $P=0.823$	0.08 $P=0.780$	0.18 $P=0.508$	0.16 $P=0.554$	0.16 $P=0.549$	0.05 $P=0.858$	-0.05 $P=0.860$	0.08 $P=0.762$

Table 3

Correlation matrix showing the relationship between daily greenhouse gas (GHG) emissions (CO₂, N₂O and CH₄) and key soil quality parameters (redox potential, NH₄⁺ and NO₃⁻) during soil recovery. Significant relationships are shown in bold.

	CH ₄	CO ₂	N ₂ O	Redox	NH ₄ ⁺
CO ₂	-0.013 <i>P</i> = 0.919				
N ₂ O	-0.17 <i>P</i> = 0.181	0.03 <i>P</i> = 0.792			
Redox	-0.56 <i>P</i> < 0.001	0.06 <i>P</i> = 0.637	0.14 <i>P</i> = 0.264		
NH ₄ ⁺	0.60 <i>P</i> < 0.001	0.01 <i>P</i> = 0.920	0.188 <i>P</i> = 0.137	-0.58 <i>P</i> < 0.001	
NO ₃ ⁻	-0.12 <i>P</i> = 0.353	-0.03 <i>P</i> = 0.802	0.11 <i>P</i> = 0.396	-0.05 <i>P</i> = 0.708	-0.06 <i>P</i> = 0.633

Figure 1
[Click here to download high resolution image](#)

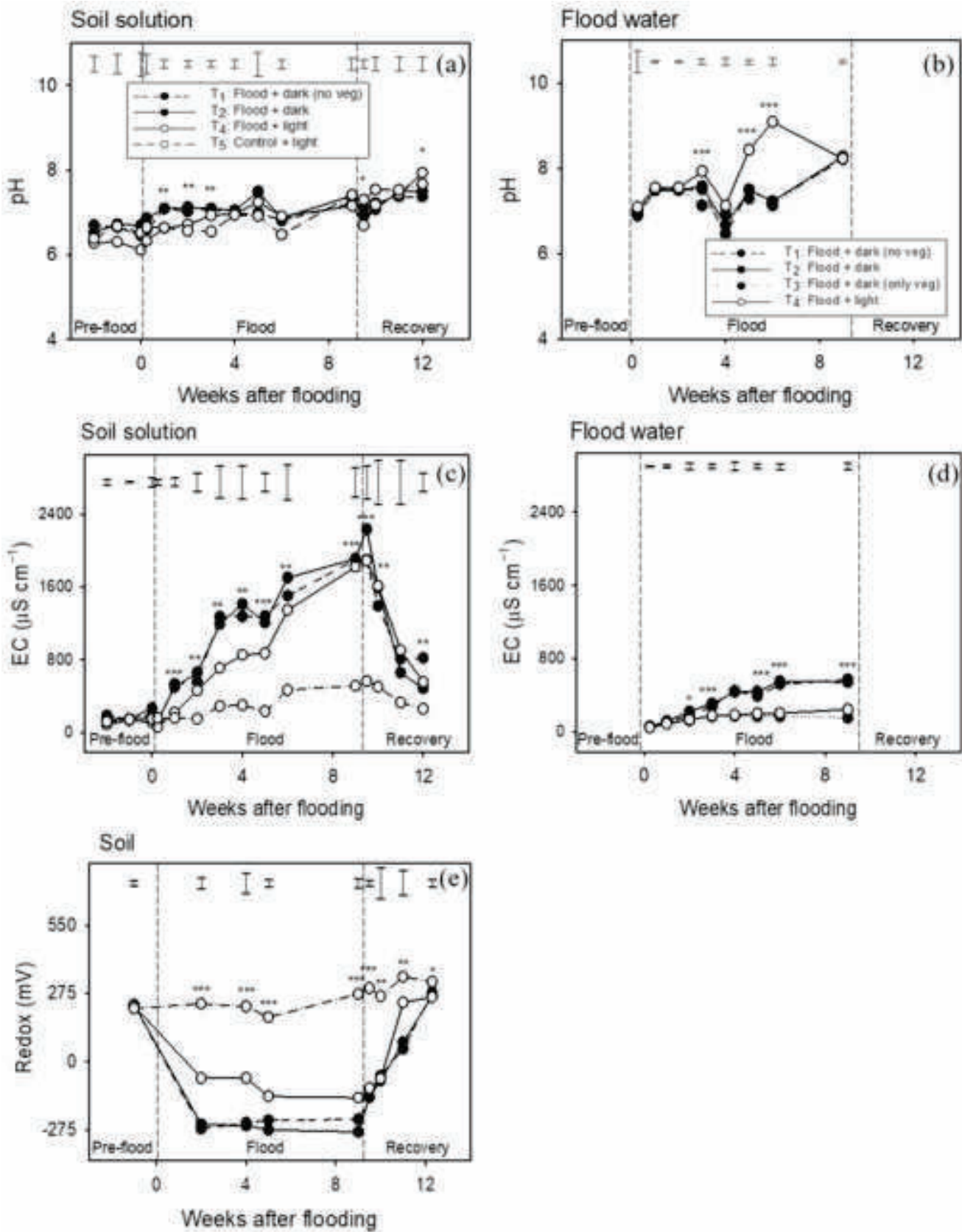


Figure 1

Figure 2
[Click here to download high resolution image](#)

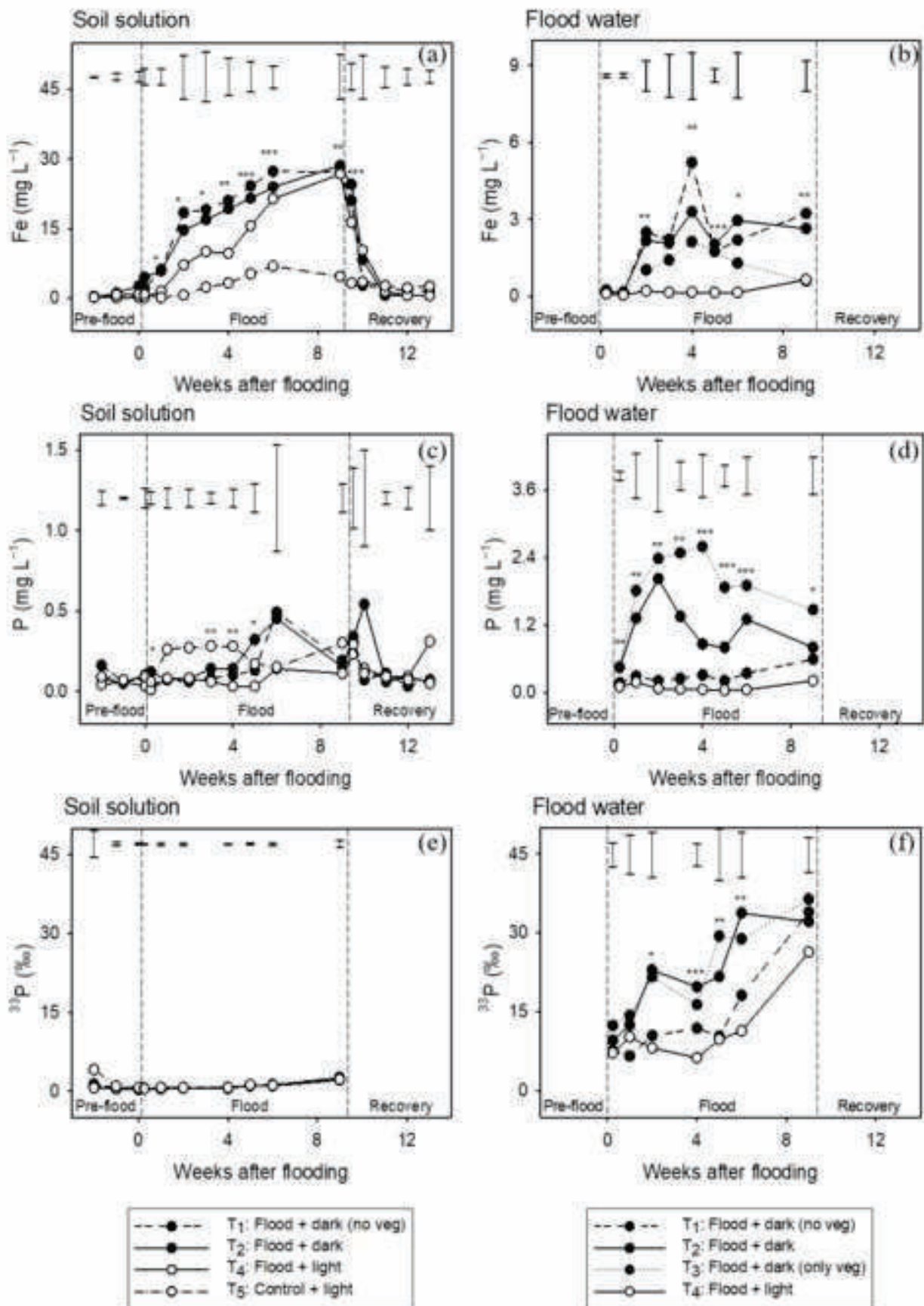


Figure 2

Figure 3
[Click here to download high resolution image](#)

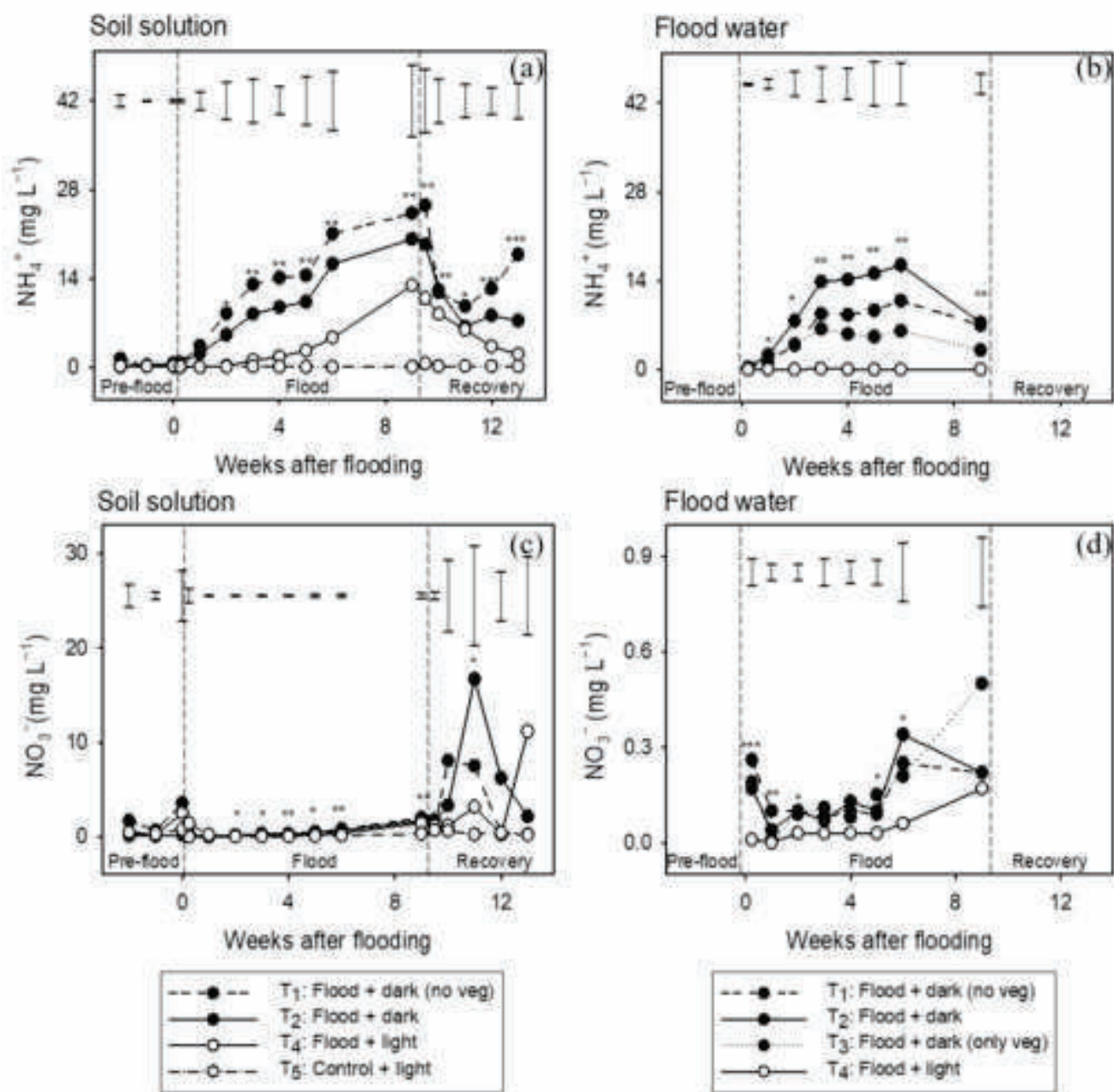


Figure 3

Figure 4
[Click here to download high resolution image](#)

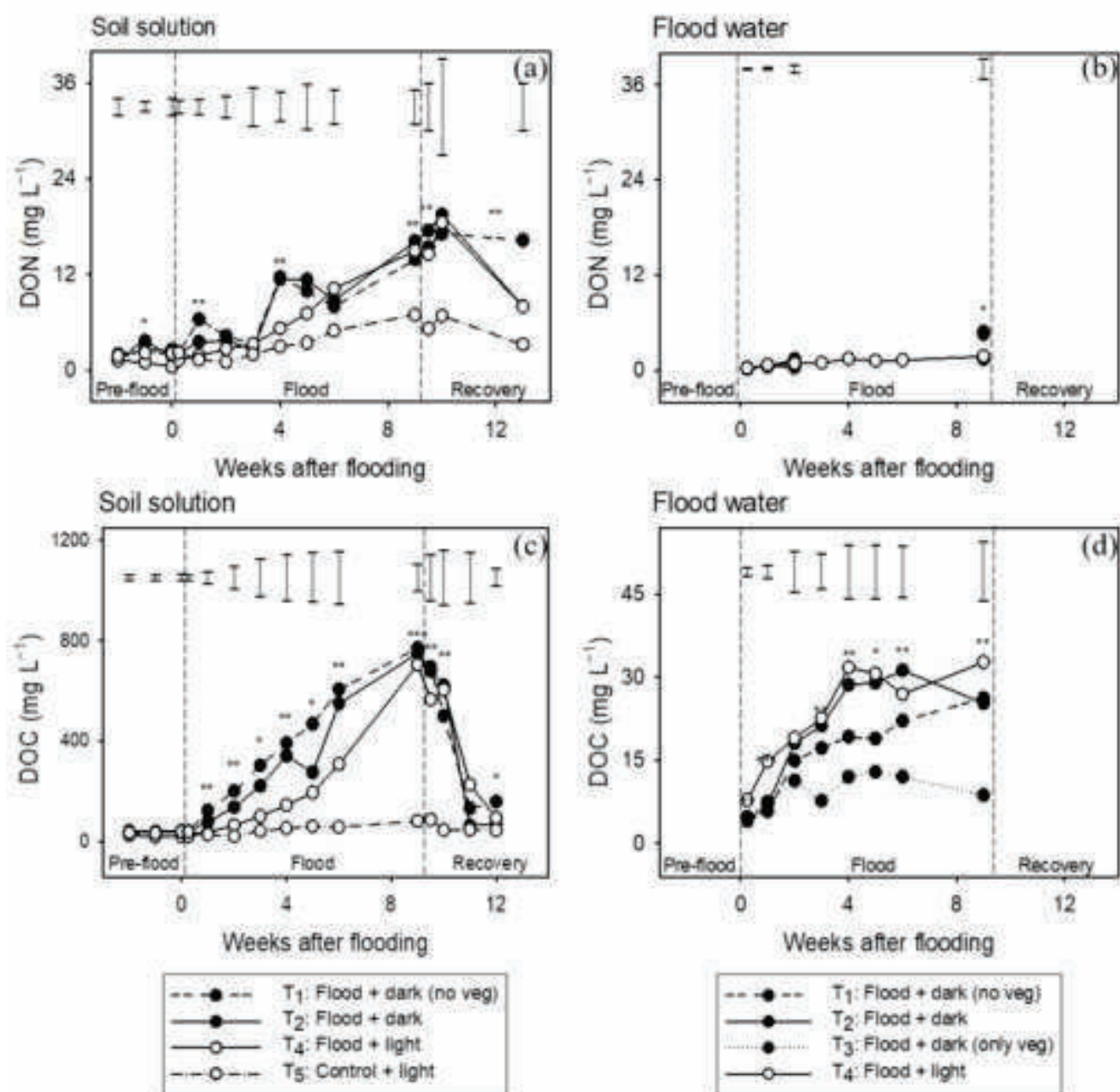


Figure 4

Figure 5
[Click here to download high resolution image](#)

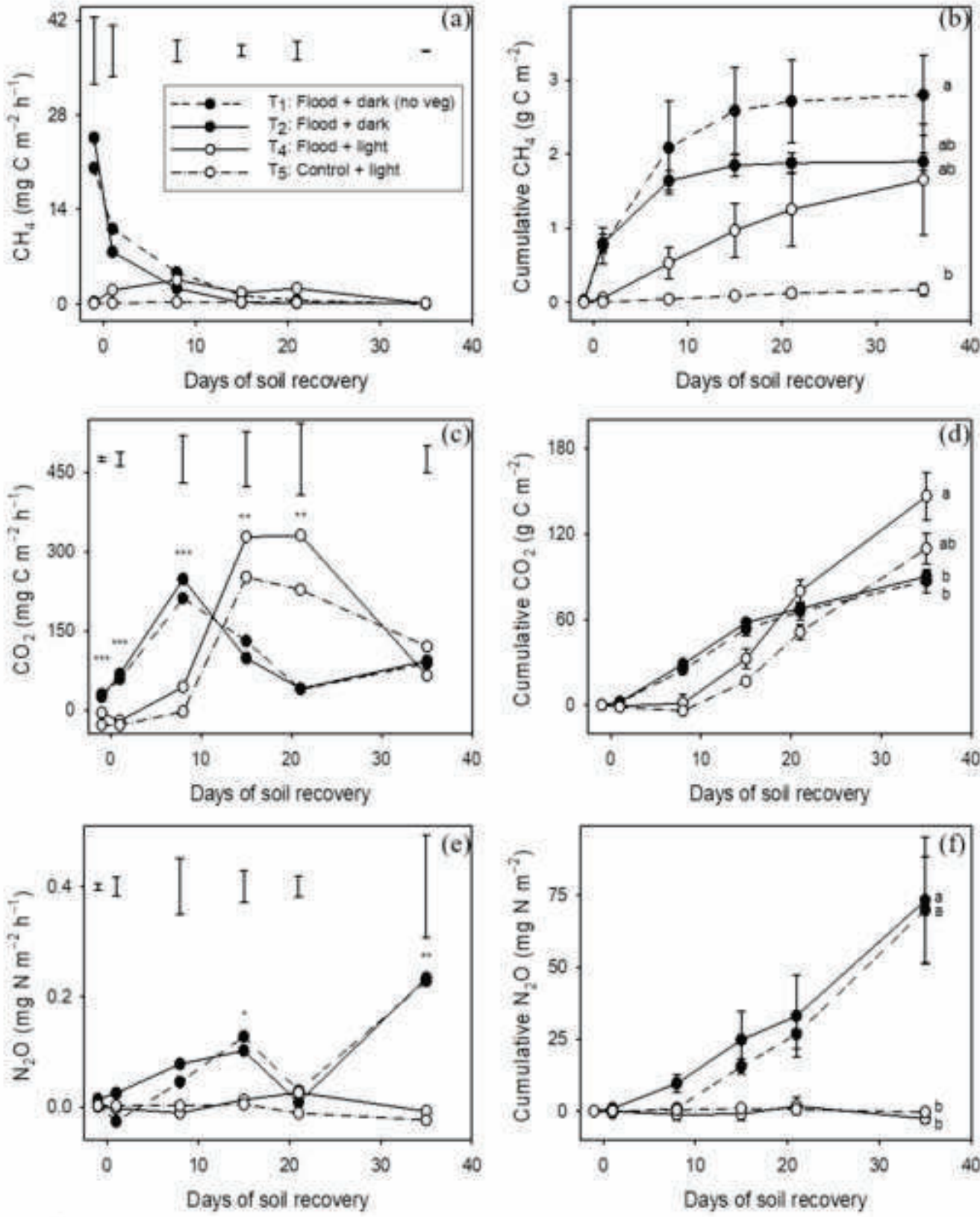


Figure 5

Figure 6
[Click here to download high resolution image](#)

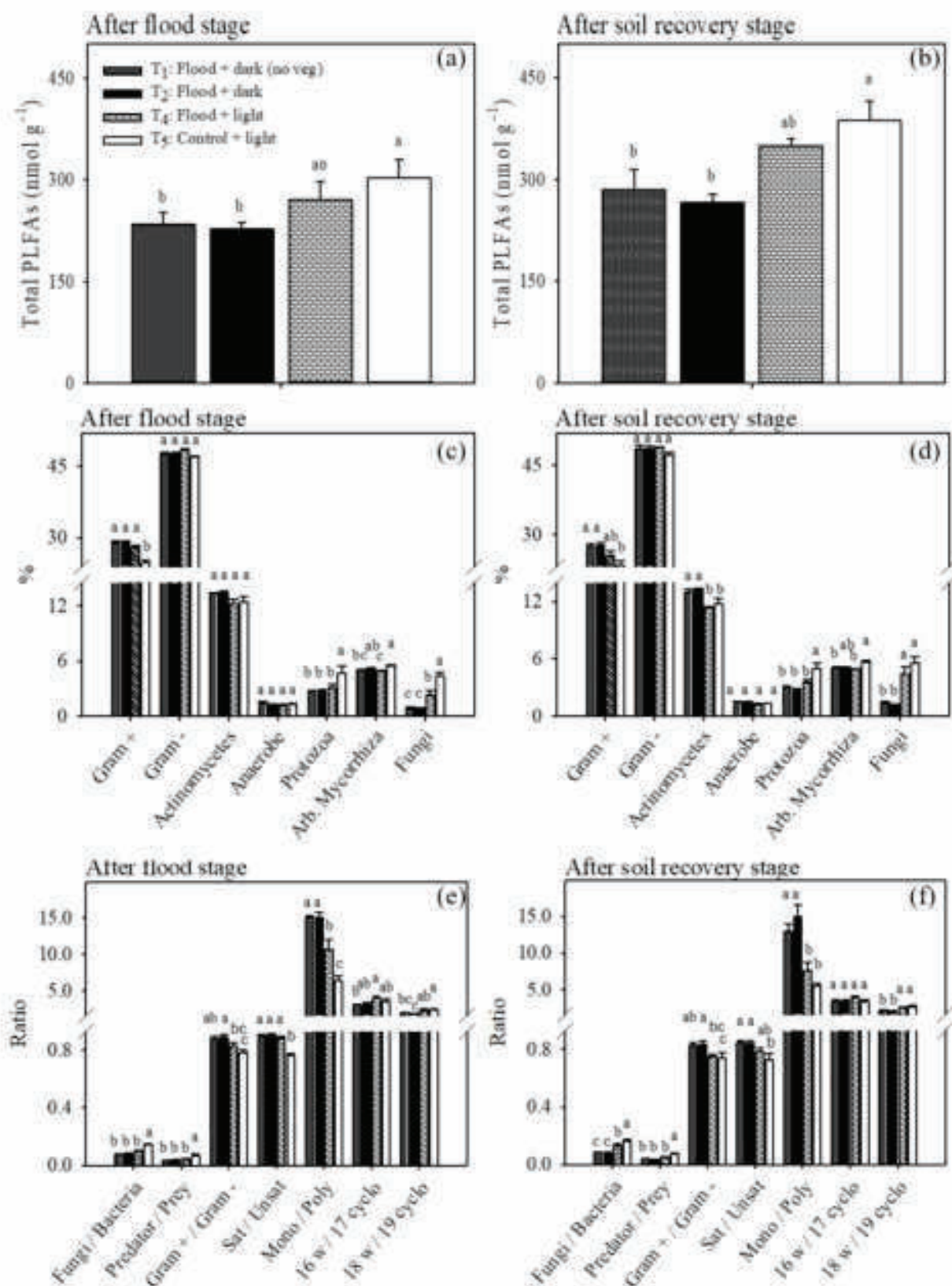


Figure 6

Figure 7
[Click here to download high resolution image](#)

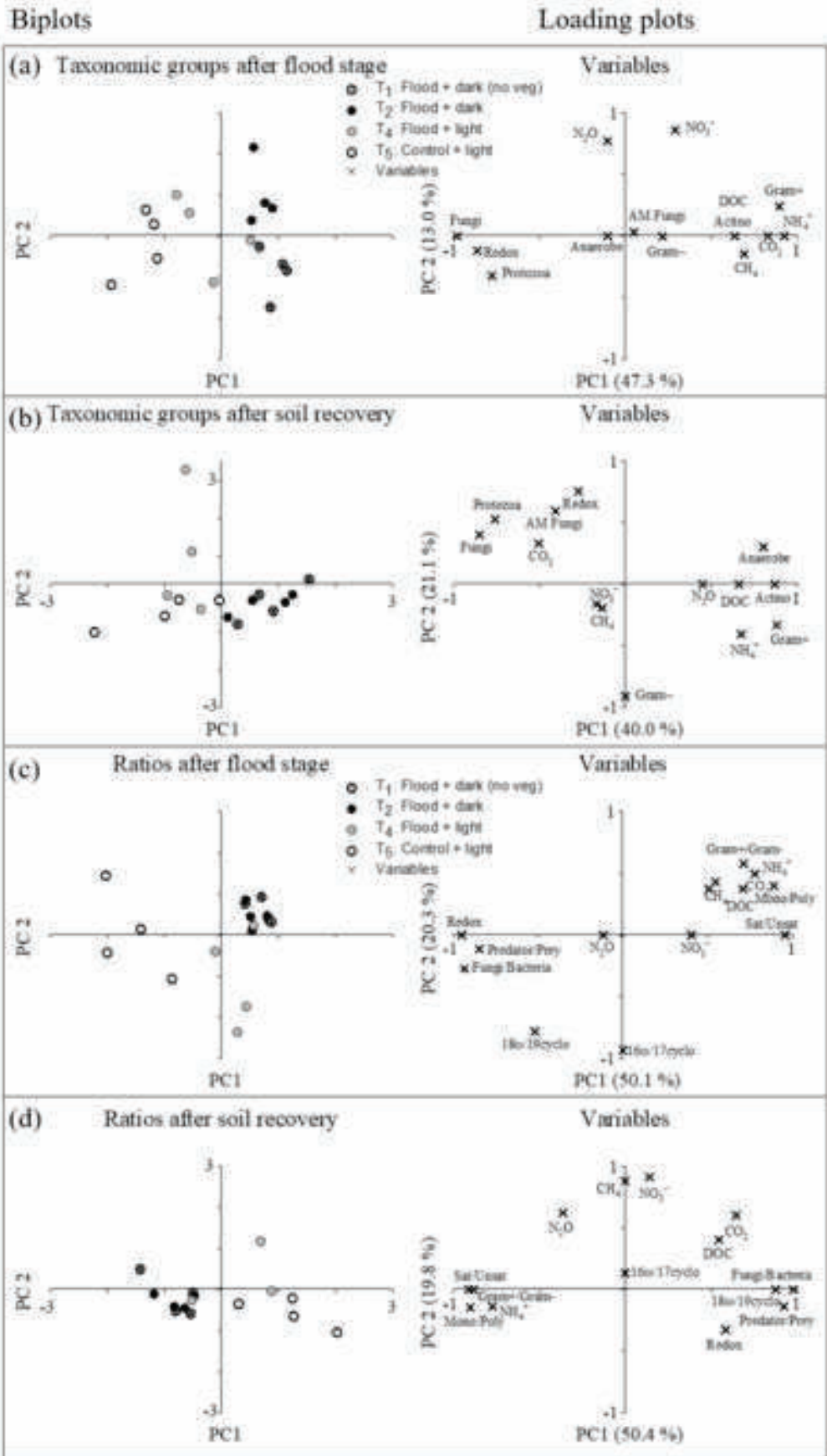


Figure 7

Supplementary Material for online publication only

[Click here to download Supplementary Material for online publication only: Supp Info DLJ.docx](#)